Encoding an oscillator into many oscillators

Kyungjoo Noh,[1,2,*] S. M. Girvin,[1,2] and Liang Jiang[1,2,†]

[1]*Departments of Applied Physics and Physics, Yale University, New Haven, Connecticut 06520, USA*
[2]*Yale Quantum Institute, Yale University, New Haven, Connecticut 06520, USA*

Gaussian errors such as excitation losses, thermal noise and additive Gaussian noise errors are key challenges in realizing large-scale fault-tolerant continuous-variable (CV) quantum information processing and therefore bosonic quantum error correction (QEC) is essential. In many bosonic QEC schemes proposed so far, a finite dimensional discrete-variable (DV) quantum system is encoded into noisy CV systems. In this case, the bosonic nature of the physical CV systems is lost at the error-corrected logical level. On the other hand, there are several proposals for encoding an infinite dimensional CV system into noisy CV systems. However, these CV-into-CV encoding schemes are in the class of Gaussian quantum error correction and therefore cannot correct practically relevant Gaussian errors due to established no-go theorems which state that Gaussian errors cannot be corrected by Gaussian QEC schemes. Here, we work around these no-go results and show that it is possible to correct Gaussian errors using GKP states as non-Gaussian resources. In particular, we propose a family of non-Gaussian quantum error-correcting codes, GKP-repetition codes, and demonstrate that they can correct additive Gaussian noise errors. In addition, we generalize our GKP-repetition codes to an even broader class of non-Gaussian QEC codes, namely, GKP-stabilizer codes and show that there exists a highly hardware-efficient GKP-stabilizer code, the two-mode GKP-squeezed-repetition code, that can quadratically suppress additive Gaussian noise errors in both the position and momentum quadratures. Moreover, for any GKP-stabilizer code, we show that logical Gaussian operations can be readily implemented by using only physical Gaussian operations. Finally, we also discuss how our GKP-stabilizer coding schemes can be used to correct Gaussian excitation losses and thermal noise as well as additive Gaussian noise errors.

I. INTRODUCTION

Harmonic oscillator modes or continuous-variable (CV) quantum systems are ubiquitous in various quantum computing and communication architectures [1, 2] and provide unique advantages, for example, to quantum simulation of bosonic systems such as boson sampling [3] and simulation of vibrational quantum dynamics of molecules [4, 5]. Since CV quantum information processing is typically implemented by using harmonic oscillator modes in photonic or phononic systems, realistic imperfections such as photon (or phonon) losses, thermal noise and dephasing noise are major challenges for realizing large-scale fault-tolerant CV quantum information processing. For example, while an ideal bosonic system may be able to exhibit quantum computational advantage over classical computers through boson sampling [3], it is unclear whether such an advantage will still remain even when a constant fraction of photons is lost [6].

Similar to the discrete-variable (DV) case [7], bosonic quantum error correction (QEC) [8] will be essential for scalable fault-tolerant CV quantum information processing. In many bosonic QEC schemes proposed so far, a finite dimensional DV system is encoded into an oscillator [9–12] or into many oscillators [13–20]. For example, in the case of a Schrödinger cat code [9, 11], a 2-dimensional logical qubit is encoded into an oscillator by using even and odd Schrödinger cat states: $|0_L\rangle \propto |\alpha\rangle + |-\alpha\rangle$ and $|1_L\rangle \propto |\alpha\rangle - |-\alpha\rangle$. Thanks to the inherent hardware efficiency, various qubit-into-an-oscillator schemes (including the Schrödinger cat code) have been realized experimentally [21–27]. However, in such

DV-into-CV QEC schemes, the bosonic nature of the physical oscillator modes is lost at the logical level because the error-corrected logical system is described by discrete variables such as Pauli operators. Therefore, the error-corrected logical DV system is not itself tailored to CV quantum information processing tasks.

On the other hand, if an infinite dimensional CV system is encoded into noisy CV systems (i.e., CV-into-CV QEC), such an error-corrected bosonic system will still be tailored to, e.g., boson sampling [3] and simulation of vibrational quantum dynamics of molecules [4, 5]. There have been several proposals for encoding an oscillator mode into many oscillators [28–34]. For example, in the case of the three-mode Gaussian-repetition code [28, 29], an infinite dimensional oscillator mode is encoded into three oscillators by repeatedly appending position eigenstates: $|\hat{q}_L = q\rangle \equiv |\hat{q}_1 = q\rangle|\hat{q}_2 = q\rangle|\hat{q}_3 = q\rangle$. Here, q can be any real number and thus the logical Hilbert space is infinite dimensional.

In general, CV-into-CV QEC is more challenging than DV-into-CV QEC because in the former we aim to protect an infinite dimensional bosonic Hilbert space against relevant errors, whereas in the latter we only aim to protect a finite dimensional Hilbert space embedded in infinite dimensional bosonic modes. Indeed, while there exist many DV-into-CV QEC schemes that can correct experimentally relevant Gaussian errors [8], none of the previously proposed CV-into-CV QEC schemes can correct Gaussian errors because they are *Gaussian quantum error correction* schemes, and established no-go theorems state that Gaussian errors cannot be corrected by Gaussian QEC schemes [20, 35, 36]. Since Gaussian errors include excitation losses, thermal noise and additive Gaussian noise errors which are ubiquitous in many realistic CV quantum systems, these no-go results set a hard limit on the practical utility of the proposed Gaussian QEC schemes.

_____

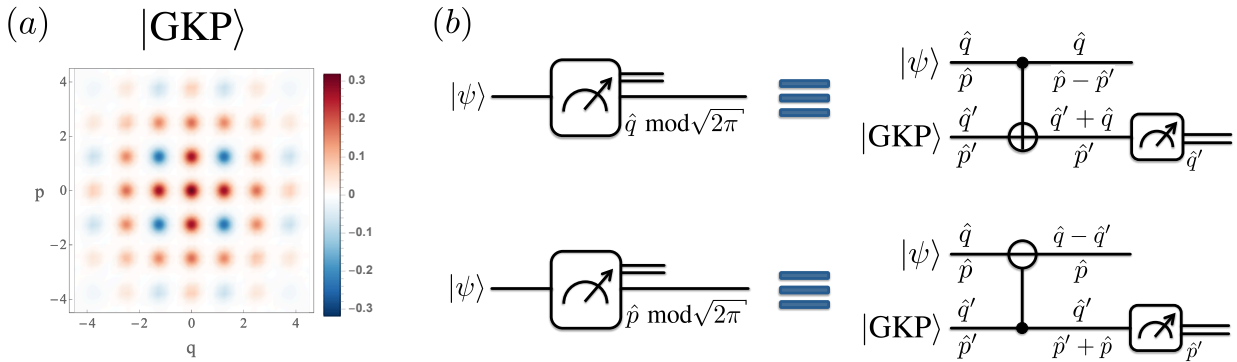* kyungjoo.noh@yale.edu
† liang.jiang@yale.edu

FIG. 1: (a) An approximate GKP state with an average photon number $\bar{n} = 5$. (b) Measurement of the position or momentum operator modulo $\sqrt{2\pi}$.

In this paper, we circumvent the established no-go results and provide *non-Gaussian* CV-into-CV QEC schemes that can correct Gaussian errors using GKP states [10] as non-Gaussian resources. Our paper is organized as follows: In Section II, we briefly review common non-Gaussian resources and summarize known properties of the GKP state that will be used in later sections. In Section III, we introduce a family of non-Gaussian CV-into-CV QEC schemes, namely, GKP-repetition codes and demonstrate that it is indeed possible to correct Gaussian errors using GKP-repetition codes. In Section IV, we generalize GKP-repetition codes and propose an even broader class of non-Gaussian QEC schemes, called GKP-stabilizer codes. In particular, in Subsection IV A, we show that there exists a highly hardware-efficient GKP-stabilizer code, the two-mode GKP-squeezed-stabilizer code, that can quadratically suppress additive Gaussian noise errors in both the position and momentum quadratures by using only one ancillary bosonic mode. In Subsection IV B, we show that, for any GKP-stabilizer codes, logical Gaussian operations can be readily implemented by using only physical Gaussian operations which are available in many experimental systems. In Section V, we briefly discuss experimental realization of our schemes and realistic imperfections.

II. GKP STATES AS NON-GAUSSIAN RESOURCES

The established no-go theorems on Gaussian QEC schemes [20, 35, 36] make it clear that non-Gaussian resources are necessary for correcting Gaussian errors while preserving the bosonic nature at the error-corrected logical level. The most common non-Gaussian resources are the single photon Fock state and photon number measurements which are useful for (error-uncorrected) universal CV quantum computation via the KLM protocol [37] and boson sampling [3]. Other useful non-Gaussian resources include Kerr non-linearity [38], cubic phase state (and gate) [10], SNAP gate [39], Schrödinger cat states [9] and GKP states [10]. Notably, GKP states have recently been shown to be valuable non-Gaussian resources which, when combined with Gaussian operations, allow fault-tolerant universal DV quantum computation via DV-into-CV GKP codes [40].

Among these non-Gaussian resources, we show that GKP states are particularly useful, not only for error-corrected DV quantum information processing, but also for error-corrected CV quantum information processing. Specifically, we use GKP states as non-Gaussian resources to construct a family of non-Gaussian CV-into-CV QEC codes that can correct various Gaussian errors while still preserving the bosonic character of the encoded system. Below, we briefly review the key properties of GKP states which will be used in later sections.

We cast the GKP state as a tool to work around the Heisenberg uncertainty principle which states that the position and momentum operators $\hat{q} \equiv (\hat{a}^\dagger + \hat{a})/\sqrt{2}$ and $\hat{p} \equiv i(\hat{a}^\dagger - \hat{a})/\sqrt{2}$ cannot be measured simultaneously because they do not commute with each other (i.e., $[\hat{q}, \hat{p}] = i \neq 0$). Despite the Heisenberg uncertainty principle, the following displacement operators

$$\hat{S}_q \equiv e^{i\sqrt{2\pi}\hat{q}} \quad \text{and} \quad \hat{S}_p \equiv e^{-i\sqrt{2\pi}\hat{p}} \tag{1}$$

do commute with each other and therefore can be measured simultaneously [10]. Since measuring $\hat{S}_q = \exp[i\sqrt{2\pi}\hat{q}]$ and $\hat{S}_p \equiv \exp[-i\sqrt{2\pi}\hat{p}]$ is equivalent to measuring their exponents $i\sqrt{2\pi}\hat{q}$ and $-i\sqrt{2\pi}\hat{p}$ modulo $2\pi i$, the commutativity of $\hat{S}_q$ and $\hat{S}_p$ implies that the position and momentum operators can indeed be measured simultaneously if they are measured modulo $\sqrt{2\pi}$. The canonical GKP state (or the grid state) [10, 41] is defined as the unique (up to an overall phase) simultaneous eigenstate of the two commuting displacement operators $\hat{S}_q$ and $\hat{S}_p$ with unit eigenvalues. Explicitly, the canonical GKP state is given by

$$|\text{GKP}\rangle \propto \sum_{n \in \mathbb{Z}} |\hat{q} = \sqrt{2\pi}n\rangle \propto \sum_{n \in \mathbb{Z}} |\hat{p} = \sqrt{2\pi}n\rangle, \tag{2}$$

and thus clearly has definite values for both the position and momentum operators modulo $\sqrt{2\pi}$, i.e., $\hat{q} = \hat{p} = 0$ mod $\sqrt{2\pi}$.

Ideally, the canonical GKP state has an infinite average photon number because it is superpositions of infinitely many ($\sum_{n \in \mathbb{Z}}$) infinitely squeezed states ($|\hat{q} = \sqrt{2\pi}n\rangle$ or $|\hat{p} = \sqrt{2\pi}n\rangle$). However, one can define an approximate GKP state
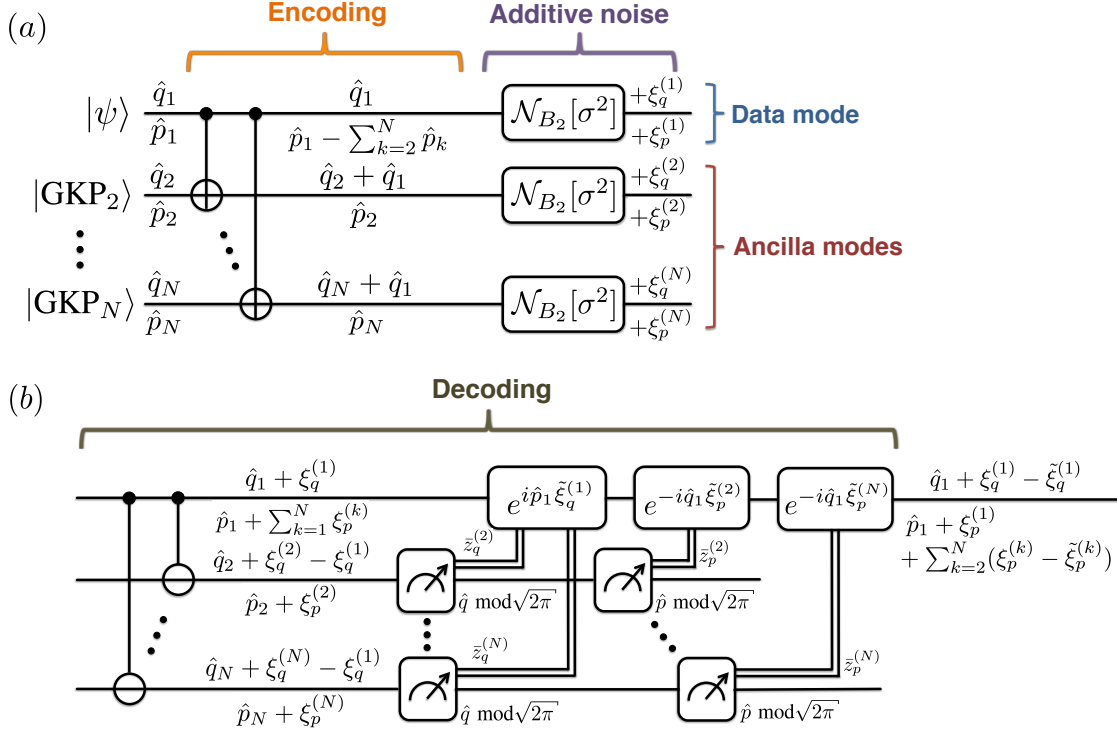
FIG. 2: (a) Encoding circuit of the N-mode GKP-repetition code subject to independent and identically distributed additive Gaussian noise errors. (b) Decoding circuit of the N-mode GKP-repetition code.

with a finite average photon number by applying a non-unitary operator $\exp[-\Delta^2 \hat{n}]$ to the canonical GKP state and then normalizing the output state: $|GKP_\Delta\rangle \propto \exp[-\Delta^2 \hat{n}]|GKP\rangle$ [10]. In Fig. 1 (a), we plot the Wigner function of the canonical GKP state with an average photon number $\bar{n} = 5$. Negative peaks in the Wigner function clearly indicate that the canonical GKP state is a non-Gaussian state.

There are many proposals for preparing a GKP state in various experimental platforms [10, 42–51]. Notably, the proposal in [42] has recently been realized in a trapped ion system [25, 26] and the one in Ref. [46] has recently been realized in a circuit QED system [27]. We also remark that such an ability to prepare the canonical GKP state allows us to measure the position (momentum) operator modulo $\sqrt{2\pi}$ when combined with the SUM (DIFFERENCE) gate and homodyne measurement of the position (momentum) operator (see Fig. 1 (b) and Ref. [10] for more details). Definitions of the SUM and DIFFERENCE gates are given below. The canonical GKP state (Fig. 1 (a)) and the modular measurements of the position and momentum operators (Fig. 1 (b)) are the key non-Gaussian resources in our CV-into-CV QEC schemes introduced below.

In the following section, we construct a family of non-Gaussian QEC codes, namely, GKP-repetition codes and demonstrate that they can correct additive Gaussian noise errors. That is, we circumvent the established no-go results on Gaussian QEC schemes [20, 35, 36] by using the canonical GKP state as a non-Gaussian resource. In Section V, we will address issues related to the use of more realistic approximate

GKP states.

III. GKP-REPETITION CODES

Quantum error-correcting codes work by hiding the quantum information from the environment by storing the logical state in a non-local entangled state of the physical components. In the case of the scheme we present below, a data oscillator mode is entangled via Gaussian operations with ancilla oscillator modes, which are initially in the canonical GKP states, in a manner that prevents the environment from learning about the logically encoded state. Like DV-into-CV GKP codes [10], our CV-into-CV QEC schemes are specifically designed to protect against random displacement errors. Also, it succeeds because we assume access to non-Gaussian resources (GKP states and modular quadrature measurements) that are unavailable to the environment.

More explicitly, we propose the following encoding of an arbitrary bosonic state $|\psi\rangle = \int dq \psi(q)|\hat{q}_1 = q\rangle$ into N oscillator modes,

$$|\psi_L\rangle = \left[\prod_{k=2}^{N} \text{SUM}_{1\to k} \right] |\psi\rangle |GKP_2\rangle \cdots |GKP_N\rangle, \quad (3)$$

and call this encoding the N-mode GKP-repetition code (see Fig. 2 (a) for the encoding circuit). We refer to the first mode as the data mode and all the other modes as the ancilla modes because the information was stored only in the

first mode before the application of the encoding circuit. $|\text{GKP}_k\rangle \propto \sum_{n \in \mathbb{Z}} |\hat{q}_k = \sqrt{2\pi}\,n\rangle$ is the canonical GKP state in the kth bosonic mode where $k \in \{2, \cdots, N\}$. The SUM gate $\text{SUM}_{j \to k} \equiv \exp[-i\hat{q}_j\hat{p}_k]$ $(j \neq k)$ is a CV analog of the DV CNOT gate which, in the Heisenberg picture, transforms $\hat{q}_k$ and $\hat{p}_j$ into $\hat{q}_k + \hat{q}_j$ and $\hat{p}_j - \hat{p}_k$ and leaves all the other quadrature operators unchanged. By the encoding circuit, the quadrature operators are transformed into

$$\hat{q}_1 \to \hat{q}_1' \equiv \hat{q}_1, \qquad \hat{p}_1 \to \hat{p}_1' \equiv \hat{p}_1 - \sum_{k=2}^{N} \hat{p}_k,$$

$$\hat{q}_k \to \hat{q}_k' \equiv \hat{q}_k + \hat{q}_1, \quad \hat{p}_k \to \hat{p}_k' \equiv \hat{p}_k, \tag{4}$$

where $k \in \{2, \cdots, N\}$. Note that the sequential application of the SUM gates in the encoding circuit is analogous to the sequence of the CNOT gates in the encoding circuit of the N-bit repetition code for qubit bit-flip errors: This is why we refer to the encoding in Eq. (3) as the N-mode GKP-repetition code.

We then assume that the oscillator modes undergo independent and identically distributed (iid) additive Gaussian noise errors (or Gaussian random displacement errors) $\mathcal{N} = \bigotimes_{k=1}^{N} \mathcal{N}_{B_2}^{(k)}[\sigma^2]$, where $\mathcal{N}_{B_2}^{(k)}[\sigma^2]$ is an additive Gaussian noise error acting on the kth mode which, in the Heisenberg picture, adds Gaussian random noises $\xi_q^{(k)}$ and $\xi_p^{(k)}$ to the position and momentum operators of the kth mode, i.e.,

$$\hat{q}_k' \to \hat{q}_k'' \equiv \hat{q}_k' + \xi_q^{(k)} \text{ and } \hat{p}_k' \to \hat{p}_k'' \equiv \hat{p}_k' + \xi_p^{(k)}. \tag{5}$$

Here, $\xi_q^{(k)}$ and $\xi_p^{(k)}$ are independent Gaussian random variables with zero mean and variance σ^2. That is, $(\xi_q^{(1)}, \xi_p^{(1)}, \cdots, \xi_q^{(N)}, \xi_p^{(N)}) \sim_{\text{iid}} \mathcal{N}(0, \sigma^2)$. The notation B_2 is based on the classification of one-mode Gaussian channels carried out in Ref. [52].

We emphasize that additive Gaussian noise errors are generic in the sense that any excitation losses and thermal noise can be converted into an additive Gaussian noise error by applying a suitable quantum-limited amplification channel [8, 53]. For example, a pure excitation loss error with loss probability γ can be converted into an additive Gaussian noise error $\mathcal{N}_{B_2}[\sigma^2]$ with $\sigma^2 = \gamma$ (see Lemma 6 and Table 1 in Ref. [53]).

The decoding procedure (shown in Fig. 2 (b)) begins with the inverse of the encoding circuit, i.e., with a sequence of DIFFERENCE$_{1 \to k}$ gates for $k \in \{2, \cdots, N\}$, where DIFFERENCE$_{1 \to k} \equiv \text{SUM}_{1 \to k}^{\dagger} = \exp[i\hat{q}_1\hat{p}_k]$. Upon the inverse of the encoding circuit, the transformed quadrature operators in Eq. (4) are transformed back to the original quadrature operators but the added quadrature noises $\xi_{q/p}^{(1)}, \cdots, \xi_{q/p}^{(N)}$ in Eq. (5) are reshaped, i.e.,

$$\hat{q}_k'' \to \hat{q}_k + z_q^{(k)}, \quad \hat{p}_k'' \to \hat{p}_k + z_p^{(k)}, \tag{6}$$

where the reshaped quadrature noises are given by

$$z_q^{(1)} \equiv \xi_q^{(1)}, \qquad z_p^{(1)} \equiv \xi_p^{(1)} + \sum_{k=2}^{N} \xi_p^{(k)},$$

$$z_q^{(k)} \equiv \xi_q^{(k)} - \xi_q^{(1)}, \qquad z_p^{(k)} \equiv \xi_p^{(k)} \tag{7}$$

for $k \in \{2, \cdots, N\}$. Note that the position quadrature noise of the data mode $\xi_q^{(1)}$ is transferred to the position quadratures of the ancilla modes (see $-\xi_q^{(1)}$ in $z_q^{(k)}$), whereas the momentum quadrature noises of the ancilla modes $\xi_p^{(k)}$ are transferred to the momentum quadrature of the data mode (see $+\sum_{k=2}^{N} \xi_p^{(k)}$ in $z_p^{(1)}$).

In the remainder of the decoding procedure, both the position and momentum quadrature noises of the ancilla modes are measured simultaneously modulo $\sqrt{2\pi}$ (using the measurement circuits shown in Fig. 1 (b)). By doing so, we measure both $\hat{q}_k''' \equiv \hat{q}_k + z_q^{(k)}$ and $\hat{p}_k''' \equiv \hat{p}_k + z_p^{(k)}$ modulo $\sqrt{2\pi}$ for all $k \in \{2, \cdots, N\}$. Note that such measurements of $\hat{q}_k'''$ and $\hat{p}_k'''$ modulo $\sqrt{2\pi}$ are equivalent to measurements of only the reshaped ancilla quadrature noises $z_q^{(k)} = \xi_q^{(k)} - \xi_q^{(1)}$ and $z_p^{(k)} = \xi_p^{(k)}$ modulo $\sqrt{2\pi}$. This is because the ancilla modes were initially in the canonical GKP state and thus $\hat{q}_k = \hat{p}_k = 0 \mod \sqrt{2\pi}$ holds for all $k \in \{2, \cdots, N\}$. The extracted information about $z_q^{(k)} = \xi_q^{(k)} - \xi_q^{(1)}$ and $z_p^{(k)} = \xi_p^{(k)}$ will then be used to estimate the data position quadrature noise $\xi_q^{(1)}$ and the ancilla momentum quadrature noises $\xi_p^{(k)}$ such that the uncertainty of the data position quadrature noise is reduced while the ancilla momentum quadrature noises (transferred to the data momentum quadrature) do not degrade the momentum quadrature of the data mode. Below, we provide a detailed description of this estimation procedure.

From the outcomes of the measurements of $z_q^{(k)}$ and $z_p^{(k)}$ modulo $\sqrt{2\pi}$, we assume that the true values of $z_q^{(k)}$ and $z_p^{(k)}$ are the ones with the smallest length among the candidates that are compatible with the modular measurement outcomes. That is,

$$\bar{z}_q^{(k)} = R_{\sqrt{2\pi}}(z_q^{(k)}) \text{ and } \bar{z}_p^{(k)} = R_{\sqrt{2\pi}}(z_p^{(k)}) \tag{8}$$

for $k \in \{2, \cdots, N\}$, where $R_s(z) \equiv z - n^{\star}(z)s$ and $n^{\star}(z) \equiv \text{argmin}_{n \in \mathbb{Z}} |z - ns|$. More concretely, $R_s(z)$ equals a displaced sawtooth function with an amplitude and period s and is given by $R_s(z) = z$ if $z \in [-s/2, s/2]$. Then, based on these estimates, we further estimate that the position quadrature noise of the data mode $\xi_q^{(1)}$ and the momentum quadrature noises of the ancilla modes $\xi_p^{(k)}$ are

$$\tilde{\xi}_q^{(1)} = -\frac{1}{N} \sum_{\ell=2}^{N} \bar{z}_q^{(\ell)} \text{ and } \tilde{\xi}_p^{(k)} = \bar{z}_p^{(k)} \tag{9}$$

for $k \in \{2, \cdots, N\}$. The latter estimate was chosen simply because $\xi_p^{(k)} = z_p^{(k)}$ and the former choice is based on a maximum likelihood estimation explained in detail in Appendix A (see also Subsection IV B). Intuitively, the former

estimate can be roughly understood as averaging the estimated values of the reshaped ancilla momentum quadrature noises $z_q^{(k)} = \xi_q^{(k)} - \xi_q^{(1)}$ such that the ancilla position quadrature noises $\xi_q^{(k)}$ are averaged out in the limit of large N.

Finally, we apply counter displacement operations $\exp[i\hat{p}_1\tilde{\xi}_q^{(1)}]$ and $\exp[-i\hat{p}_1\sum_{k=2}^{N}\tilde{\xi}_p^{(k)}]$ to the data mode based on the above estimates and end up with the following logical position and momentum quadrature noises

$$\xi_q \equiv z_q^{(1)} - \tilde{\xi}_q^{(1)} = \xi_q^{(1)} + \frac{1}{N}\sum_{k=2}^{N}R_{\sqrt{2\pi}}(\xi_q^{(k)} - \xi_q^{(1)}),$$

$$\xi_p \equiv z_p^{(1)} - \sum_{k=2}^{N}\tilde{\xi}_p^{(k)} = \xi_p^{(1)} + \sum_{k=2}^{N}(\xi_p^{(k)} - R_{\sqrt{2\pi}}(\xi_p^{(k)})).$$

$$(10)$$

In Appendix B, we provide explicit expressions for the probability density functions of ξ_q and ξ_p (which are used to obtain Fig. 3) in the most general case. Here, we instead focus on a simple (but important) case where σ is much smaller than $\sqrt{2\pi}$. In this case, the reshaped ancilla quadrature noises $z_q^{(k)} = \xi_q^{(k)} - \xi_q^{(1)}$ and $z_p^{(k)} = \xi_p^{(k)}$ lie in the unambiguously distinguishable range $[-\sqrt{\pi/2}, \sqrt{\pi/2}]$ with a very high probability and thus we have $R_{\sqrt{2\pi}}(\xi_q^{(k)} - \xi_q^{(1)}) = \xi_q^{(k)} - \xi_q^{(1)}$ and $R_{\sqrt{2\pi}}(\xi_p^{(k)}) = \xi_p^{(k)}$. Then, the logical position and momentum quadrature noises are given by

$$\xi_q \xrightarrow{\sigma \ll \sqrt{2\pi}} \frac{1}{N}\sum_{k=1}^{N}\xi_q^{(k)} \sim \mathcal{N}\left(0, \sigma_q^2 = \frac{\sigma^2}{N}\right),$$

$$\xi_p \xrightarrow{\sigma \ll \sqrt{2\pi}} \xi_p^{(1)} \sim \mathcal{N}\left(0, \sigma_p^2 = \sigma^2\right),$$

$$(11)$$

That is, the variance of the logical position quadrature noise is reduced by a factor of N. This is due to the syndrome measurements of the reshaped ancilla position quadrature noises $z_q^{(k)} = \xi_q^{(k)} - \xi_q^{(1)}$ modulo $\sqrt{2\pi}$ (for all $k \in \{2, \cdots, N\}$) which are then used to reduce the uncertainty of the data position quadrature noise $\xi_q^{(1)}$. Moreover, the variance of the logical momentum quadrature noise remains unchanged despite the temporary increase ($\xi_p^{(1)} \rightarrow z_p^{(1)} = \xi_p^{(1)} + \sum_{k=2}^{N}\xi_p^{(k)}$) during the decoding procedure. Again, this is due to the syndrome measurements of the reshaped ancilla momentum quadrature noises $z_p^{(k)} = \xi_p^{(k)}$ modulo $\sqrt{2\pi}$ which fully capture the transferred ancilla momentum quadrature noises $\xi_p^{(k)}$ for all $k \in \{2, \cdots, N\}$ if $\sigma \ll \sqrt{2\pi}$.

In Fig. 3, we plot the standard deviations of the logical quadrature noises for the two-mode GKP-repetition code (i.e., $N = 2$). The standard deviation of the logical position quadrature noise is indeed reduced by a factor of $\sqrt{N} = \sqrt{2}$ (i.e., $\sigma_q = \sigma/\sqrt{2}$), while the standard deviation of the logical momentum quadrature noise remains unchanged (i.e., $\sigma_p = \sigma$) for $\sigma \lesssim 0.3$. Note that the condition $\sigma \lesssim 0.3$ is translated to $\gamma = \sigma^2 \lesssim 0.1$ in the case of pure excitation losses, where γ is the pure-loss probability [8, 53]. Thus,
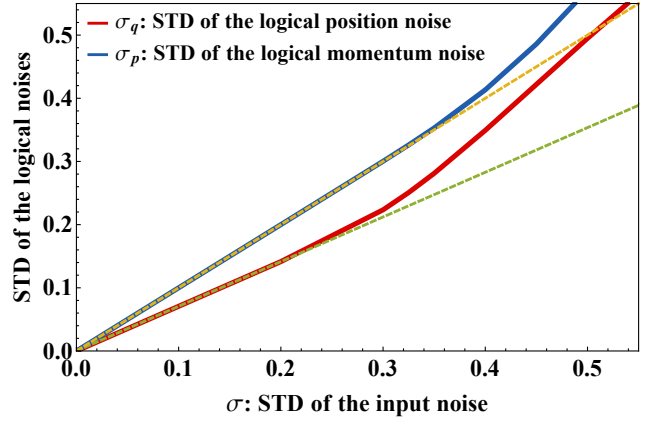

FIG. 3: Standard deviations of the logical quadrature noises σ_q and σ_p as a function of the input standard deviation σ for the two-mode GKP-repetition code (i.e., $N = 2$). The green and yellow dashed lines represent $\sigma_q = \sigma/\sqrt{2}$ and $\sigma_p = \sigma$.

if the standard deviation of an additive Gaussian noise error is sufficiently small, our GKP-repetition coding scheme can successfully reduce the noise of the position quadrature, while keeping the momentum quadrature noise unchanged. That is, our (non-Gaussian) GKP-repetition codes can *correct* additive Gaussian noise errors.

We remark that in an analogous N-mode Gaussian-repetition coding scheme (presented in detail in Appendix A), the variance of the position quadrature noise is reduced by a factor of N (i.e., $\sigma_q^2 = \sigma^2/N$) as in Eq. (11) but the variance of the momentum quadrature noise is increased by the same factor (i.e., $\sigma_p^2 = N\sigma^2$). This implies that, in the case of Gaussian-repetition codes, the quadrature noises are only squeezed ($\sigma_q\sigma_p = \sigma^2$) instead of being corrected ($\sigma_q\sigma_p < \sigma^2$): This reaffirms the previous no-go results on Gaussian QEC schemes [20, 35, 36].

The key difference between our GKP-repetition codes and the previous Gaussian-repetition codes is that, in the latter case, the ancilla momentum quadrature noises that are transferred to the data mode (see $+\sum_{k=2}^{N}\xi_p^{(k)}$ in $z_p^{(1)}$) are left completely undetected, whereas in the former case they are captured by measuring the ancilla momentum quadrature operations modulo $\sqrt{2\pi}$. Such a limitation of Gaussian-repetition codes is in fact a general feature of any Gaussian QEC scheme which relies on homodyne measurements of quadrature operators. With homodyne measurements, one can only monitor the noise of one quadrature of a bosonic mode, while the other conjugate quadrature noise is left completely undetected.

On the other hand, we have worked around this barrier by using the canonical GKP state as a non-Gaussian resource which allows simultaneous measurements of both the position and momentum quadrature operators modulo $\sqrt{2\pi}$ (see Fig. 1). In this regard, we emphasize that such non-Gaussian modular simultaneous measurements of both position and momentum quadrature operators (using canonical GKP states) are fundamentally different from Gaussian heterodyne measurements [54] where both quadrature operators are measured

simultaneously but in a necessarily noisy manner.

Finally, we compare our GKP-repetition codes with the conventional multi-qubit repetition codes (i.e., $|0_L\rangle = |0\rangle^{\otimes N}$ and $|1_L\rangle = |1\rangle^{\otimes N}$) which can correct qubit bit-flip errors [55]. First, we observe that only two bosonic modes ($N = 2$) are sufficient to reduce the variance of the position quadrature noise in the case of GKP-repetition codes, whereas at least three qubits are needed to suppress qubit bit-flip errors in the case of mutli-qubit repetition codes. However, while GKP-repetition codes can be implemented in a more hardware-efficient way, they do not reduce the variance of the position quadrature noise quadratically but instead only reduced the variance by a constant factor N. On the other hand, the three-qubit repetition code can reduce the bit-flip error probability quadratically from p to $p_L \simeq 3p^2$ if $p \ll 1$.

Given that such a quadratic (or even higher order) suppression of errors was a key step towards fault-tolerant universal DV quantum computation [7], it is also highly desirable in the CV case to have such a quadratic suppression of additive Gaussian noise errors going way beyond the reduction by a constant factor which was shown above.

Below, we introduce the two-mode GKP-squeezed-repetition code by adding single-mode squeezing operations to the two-mode GKP-repetition code and show that it can suppress the quadrature noises quadratically. In particular, the modified scheme can achieve such a quadratic noise suppression by using only two bosonic modes (one data mode and one ancilla mode) and therefore is hardware-efficient. In the DV case, on the contrary, at least five qubits and high-weight multi-qubit gate operations are needed to suppress both the bit-flip and phase-flip errors quadratically [56, 57].

IV. GENERALIZATIONS OF GKP-REPETITION CODES

In this section, we generalize our GKP-repetition codes. Specifically, in Subsection IV A, we introduce the two-mode GKP-squeezed-repetition code and show that it can suppress both the position and momentum quadrature noises quadratically. In Subsection IV B, we further generalize our QEC schemes and provide an even broader class of non-Gaussian quantum error-correcting codes, namely, GKP-stabilizer codes. We also show that logical Gaussian operations can be readily implemented by using only physical Gaussian operations for any GKP-stabilizer code.

A. The two-mode GKP-squeezed-repetition code

We define the two-mode GKP-squeezed-repetition code as follows:

$$|\psi_L\rangle = \mathrm{Sq}_1\left(\frac{1}{\lambda}\right)\mathrm{Sq}_2(\lambda)\mathrm{SUM}_{1\to 2}|\psi\rangle|\mathrm{GKP}_2\rangle, \quad (12)$$

where $|\psi\rangle = \int dq\, \psi(q)|\hat{q}_1 = q\rangle$ is an arbitrary bosonic state and $\mathrm{Sq}_k(\lambda)$ is the single-mode squeezing operation acting on the kth mode and transforms $\hat{q}_k$ and $\hat{p}_k$ into $\lambda\hat{q}_k$ and $\hat{p}_k/\lambda$ (see

Fig. 4 (a) for the encoding circuit). Note that the squeezing parameter λ is a free parameter that can be chosen at will.

The action of the encoding circuit of the two-mode GKP-squeezed-repetition code can be described by a symplectic transformation $\hat{\boldsymbol{x}}' = \boldsymbol{S}\hat{\boldsymbol{x}}$, where $\hat{\boldsymbol{x}} = (\hat{q}_1, \hat{p}_1, \hat{q}_2, \hat{p}_2)^T$ and $\hat{\boldsymbol{x}}' = (\hat{q}_1', \hat{p}_1', \hat{q}_2', \hat{p}_2')^T$ are the original and transformed quadrature operators, and the symplectic matrix $\boldsymbol{S}$ is given by

$$\boldsymbol{S} = \begin{bmatrix} 1/\lambda & 0 & 0 & 0 \\ 0 & \lambda & 0 & -\lambda \\ \lambda & 0 & \lambda & 0 \\ 0 & 0 & 0 & 1/\lambda \end{bmatrix}. \quad (13)$$

Upon the independent and identically distributed additive Gaussian noise errors, the quadrature operator $\hat{\boldsymbol{x}}'$ is further transformed into $\hat{\boldsymbol{x}}'' = \hat{\boldsymbol{x}}' + \boldsymbol{\xi}$, where $\boldsymbol{\xi} = (\xi_q^{(1)}, \xi_p^{(1)}, \xi_q^{(2)}, \xi_p^{(2)})^T$ is the quadrature noise vector that satisfies $(\xi_q^{(1)}, \xi_p^{(1)}, \xi_q^{(2)}, \xi_p^{(2)}) \sim_{\text{iid}} \mathcal{N}(0, \sigma^2)$. Then, the inverse of the encoding circuit in the decoding procedure (shown in Fig. 4 (b)) transforms the quadrature operator into $\hat{\boldsymbol{x}}''' = \boldsymbol{S}^{-1}\hat{\boldsymbol{x}}'' = \hat{\boldsymbol{x}} + \boldsymbol{z}$, where $\boldsymbol{z} \equiv (z_q^{(1)}, z_p^{(1)}, z_q^{(2)}, z_p^{(2)})^T$ is the reshaped quadrature noise vector which is given by

$$\boldsymbol{z} = \boldsymbol{S}^{-1}\boldsymbol{\xi} = \begin{bmatrix} \lambda\xi_q^{(1)} \\ \xi_p^{(1)}/\lambda + \lambda\xi_p^{(2)} \\ -\lambda\xi_q^{(1)} + \xi_q^{(2)}/\lambda \\ \lambda\xi_p^{(2)} \end{bmatrix} \equiv \begin{bmatrix} z_q^{(1)} \\ z_p^{(1)} \\ z_q^{(2)} \\ z_p^{(2)} \end{bmatrix}. \quad (14)$$

Similarly as in the case of GKP-repetition codes, information about the reshaped ancilla quadrature noises $z_q^{(2)} = -\lambda\xi_q^{(1)} + \xi_q^{(2)}/\lambda$ and $z_p^{(2)} = \lambda\xi_p^{(2)}$ are extracted by simultaneously measuring the position and momentum quadrature operators of the ancilla mode modulo $\sqrt{2\pi}$ (see Fig. 4 (b)).

Before elaborating the detailed estimation strategy from the obtained syndrome measurement outcomes, let us briefly explain the key idea behind it. Assume $\lambda > 1$ and note that the data position quadrature noise is amplified by a factor of λ (i.e., $z_q^{(1)} = \lambda\xi_q^{(1)}$) after the noise reshaping in the decoding procedure. On the other hand, the data momentum quadrature noise is shrunken by the same factor (see $\xi_p^{(1)}/\lambda$ in $z_p^{(2)}$) but there is an added noise transferred from the ancilla mode (see $+\lambda\xi_p^{(2)}$ in $z_p^{(2)}$). Then, by measuring the reshaped ancilla position quadrature noise $z_q^{(2)} = -\lambda\xi_q^{(1)} + \xi_q^{(2)}/\lambda$ modulo $\sqrt{2\pi}$, we can extract information about the amplified data position quadrature noise $\lambda\xi_q^{(1)}$ modulo $\sqrt{2\pi}$ up to a small noise $\xi_q^2/\lambda \sim \mathcal{N}(0, \sigma^2/\lambda^2)$. Using this information, we can then reduce the variance of the position quadrature noise roughly by a factor of λ^2. Similarly, by measuring the reshaped ancilla momentum quadrature noise $z_p^{(2)} = \lambda\xi_p^{(2)}$ modulo $\sqrt{2\pi}$, we can extract information about the amplified ancilla momentum quadrature noise $\lambda\xi_p^{(2)}$ which is transferred to the data mode. Then, based on this information we can remove the transferred ancilla momentum quadrature noise and are left with the shrunken data momentum quadrature noise $\xi_p^{(1)}/\lambda$. Thus, we can also reduce the variance of the momentum quadrature
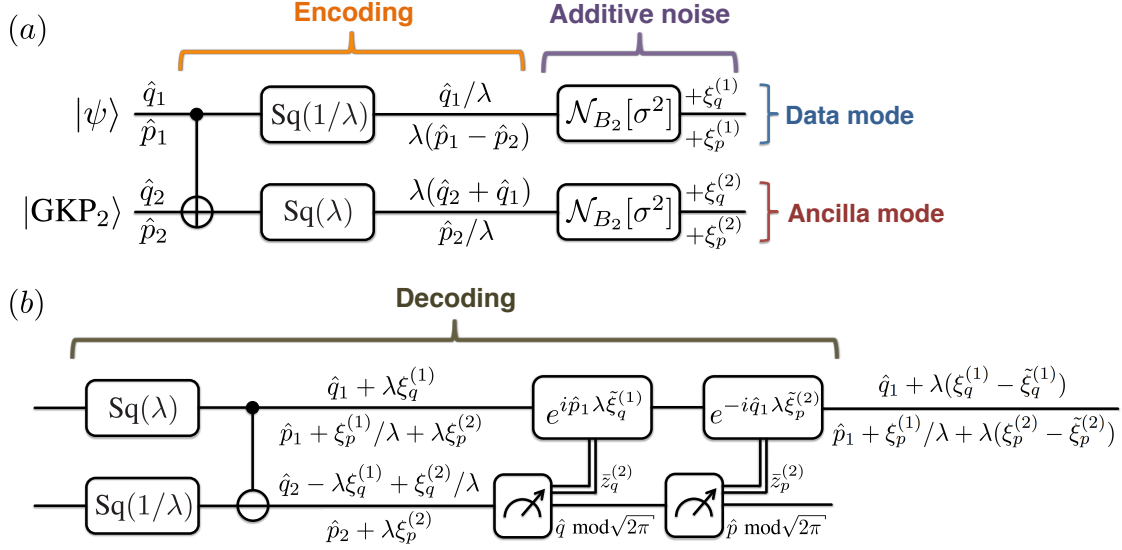
FIG. 4: (a) Encoding circuit of the two-mode GKP-squeezed-repetition code subject to independent and identically distributed additive Gaussian noise errors. (b) Decoding circuit of the two-mode GKP-squeezed-repetition code.

noise by a factor of λ^2.

Since we can reduce the variances of both the position and momentum quadrature noises by a factor of λ^2, we may want to choose $\lambda \gg 1$. However, we cannot increase λ indefinitely because then the reshaped ancilla quadrature noises $z_q^{(2)}$ and $z_p^{(2)}$ will not be contained within the unambiguously distinguishable range $[-\sqrt{\pi/2}, \sqrt{\pi/2}]$. Therefore, we have to choose λ such that the reshaped ancilla quadrature noises lie mostly in the unambiguously distinguishable range. Below, we describe this decoding strategy in more detail.

Based on the outcomes of the measurements of the ancilla quadrature operators modulo $\sqrt{2\pi}$, we estimate that the reshaped ancilla quadrature noises are

$$\bar{z}_q^{(2)} = R_{\sqrt{2\pi}}(z_q^{(2)}) \text{ and } \bar{z}_p^{(2)} = R_{\sqrt{2\pi}}(z_p^{(2)}), \quad (15)$$

similarly as in Eq. (8). Then, we further estimate that $\lambda\xi_q^{(1)}$ and $\lambda\xi_p^{(2)}$ are

$$\lambda\tilde{\xi}_q^{(1)} = -\frac{\lambda^4}{1+\lambda^4}\bar{z}_q^{(2)} \text{ and } \lambda\tilde{\xi}_p^{(2)} = \bar{z}_p^{(2)}. \quad (16)$$

The latter estimate was chosen simply because $\lambda\xi_p^{(2)} = z_p^{(2)}$ and the former estimate is based on a maximum likelyhood estimation which is discussed in detail in Appendix C (see also Subsection IV B). Finally, applying the counter displacement operations $\exp[i\hat{p}_1\lambda\tilde{\xi}_q^{(1)}]$ and $\exp[-i\hat{q}_1\lambda\tilde{\xi}_p^{(2)}]$ we end up with the logical quadrature noises

$$\xi_q \equiv z_q^{(1)} - \lambda\tilde{\xi}_q^{(1)} = \lambda\xi_q^{(1)} + \frac{\lambda^4}{1+\lambda^4}R_{\sqrt{2\pi}}\left(\frac{\xi_q^{(2)}}{\lambda} - \lambda\xi_q^{(1)}\right),$$

$$\xi_p \equiv z_p^{(1)} - \lambda\tilde{\xi}_p^{(1)} = \frac{\xi_p^{(1)}}{\lambda} + \lambda\xi_p^{(2)} - R_{\sqrt{2\pi}}(\lambda\xi_p^{(2)}). \quad (17)$$

The probability density functions of these logical quadrature noises are analyzed in detail in Appendix C assuming the most general case. Here, we instead focus on an important special case where both $\sqrt{\lambda^2 + 1/\lambda^2}\sigma$ and $\lambda\sigma$ are much smaller than $\sqrt{2\pi}$. In this case, the reshaped ancilla quadrature noises $z_q^{(2)} = -\lambda\xi_q + \xi_q^{(2)}/\lambda$ and $z_p^{(2)} = \lambda\xi_p^{(2)}$ are confined within the unambiguously distinguishable range $[-\sqrt{\pi/2}, \sqrt{\pi/2}]$ with a very high probability.

Recall that we can freely choose the squeezing parameter λ. Here, we choose $\lambda = \sqrt{2\pi}c/\sigma$ where $c \ll 1$ is a small constant. For example, c can be chosen to be $c = 0.1$. Under this choice, $\lambda\sigma = \sqrt{2\pi}c$ is guaranteed to be much smaller than $\sqrt{2\pi}$ and therefore the reshaped ancilla momentum quadrature noise $z_p^{(2)} = \lambda\xi_p^{(2)}$ will lie in the range $[-\sqrt{\pi/2}, \sqrt{\pi/2}]$ with a very high probability, yielding $R_{\sqrt{2\pi}}(\lambda\xi_p^{(2)}) = \lambda\xi_p^{(2)}$. If $\sigma \lesssim \sqrt{2\pi}c$ holds in addition to $c \ll 1$, we also have $\sqrt{\lambda^2 + 1/\lambda^2}\sigma \lesssim \sqrt{4\pi}c \ll \sqrt{2\pi}$ and therefore the reshaped ancilla position quadrature noise $z_q^{(2)} = -\lambda\xi_q^{(1)} + \xi_q^{(2)}/\lambda$ will also lie in the range $[-\sqrt{\pi/2}, \sqrt{\pi/2}]$ with a very high probability, yielding $R_{\sqrt{2\pi}}(\xi_q^{(2)}/\lambda - \lambda\xi_q^{(1)}) = \xi_q^{(2)}/\lambda - \lambda\xi_q^{(1)}$. Note that, for example, the condition $\sigma \lesssim \sqrt{2\pi}c$ is given by $\sigma \lesssim 0.25$ if we choose $c = 0.1$.

Since $R_{\sqrt{2\pi}}(\xi_q^{(2)}/\lambda - \lambda\xi_q^{(1)}) = \xi_q^{(2)}/\lambda - \lambda\xi_q^{(1)}$ and $R_{\sqrt{2\pi}}(\lambda\xi_p^{(2)}) = \lambda\xi_p^{(2)}$ hold under the above conditions (i.e., $\lambda = \sqrt{2\pi}c/\sigma$ with $c \ll 1$ and $\sigma \lesssim \sqrt{2\pi}c$), the logical quadrature noises in Eq. (17) simplify to

$$\xi_q \xrightarrow[\sigma \lesssim \sqrt{2\pi}c]{c \ll 1} \frac{\lambda\xi_q^{(1)} + \lambda^3\xi_q^{(2)}}{1+\lambda^4} \sim \mathcal{N}\left(0, \sigma_q^2 = \frac{\lambda^2\sigma^2}{1+\lambda^4}\right),$$

$$\xi_p \xrightarrow{c \ll 1} \frac{\xi_p^{(1)}}{\lambda} \sim \mathcal{N}\left(0, \sigma_p^2 = \frac{\sigma^2}{\lambda^2}\right). \quad (18)$$

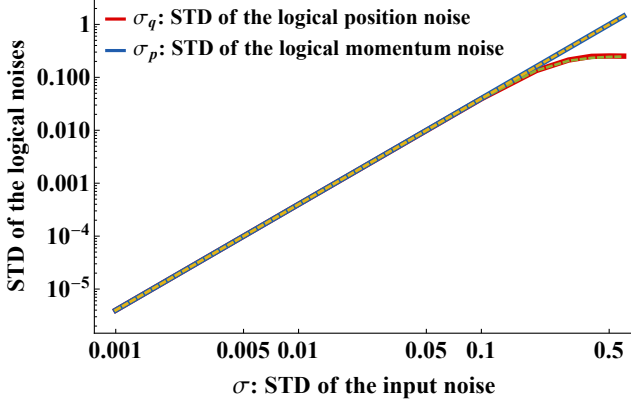FIG. 5: Standard deviations of the logical quadrature noises σ_q and σ_p as a function of the input standard deviation σ for the two-mode GKP-squeezed-repetition code. λ was chosen to be $\lambda = \sqrt{2\pi}c/\sigma$ with $c = 0.1$. The dashed green and yellow lines represent $\sigma_q = \lambda\sigma/\sqrt{1+\lambda^4} \xrightarrow{\lambda \gg 1} \sqrt{\pi/50}\,\sigma^2$ and $\sigma_p = \sigma/\lambda = \sqrt{\pi/50}\,\sigma^2$, respectively.

If the standard deviation of the input additive Gaussian noise error is sufficiently small (i.e., $\sigma \ll \sqrt{2\pi}c$), $\lambda \gg 1$ holds and the standard deviations of the logical quadrature noises in Eq. (18) are reduced by a factor of λ as explained informally above:

$$\sigma_q, \sigma_p \xrightarrow[\sigma \ll \sqrt{2\pi}c]{c \ll 1} \frac{\sigma}{\lambda} = \frac{\sigma^2}{2\pi c} \propto \sigma^2. \tag{19}$$

That is, the two-mode GKP-squeezed-repetition code can suppress both the position and momentum quadrature noises *quadratically*.

In Fig. 5, we choose $\lambda = \sqrt{2\pi}c/\sigma$ with $c = 0.1$ and plot the standard deviations σ_q and σ_p of the logical position and momentum quadrature noises as a function of the input standard deviation σ. As indicated by the agreement among the red, blue, dashed green and dashed yellow lines in Fig. 5, the quadratic noise suppression analytically derived in Eq. (19) do indeed hold when $\sigma \lesssim \sqrt{2\pi}c = 0.25 \cdots$. The condition $\sigma \lesssim 0.25$ corresponds to $\gamma = \sigma^2 \lesssim 0.06$ for the pure excitation loss errors, where γ is the loss probability. We again emphasize that our scheme is hardware-efficient because only two bosonic modes (one data mode and one ancilla mode) are needed to achieve the quadratic suppression of both quadrature noises.

B. GKP-stabilizer codes

In this subsection, we further generalize GKP-repetition codes (Section III) and the two-mode GKP-squeezed-repetition code (Subsection IV A) to an even broader class of non-Gaussian quantum error-correcting codes, namely, GKP-stabilizer codes: We define logical code states of a general GKP-stabilizer code (encoding M oscillator modes into N os-

cillator modes) as

$$|\Psi_L\rangle = \hat{U}_G^{\mathrm{Enc}}|\Psi\rangle|\mathrm{GKP}_{M+1}\rangle \cdots |\mathrm{GKP}_N\rangle, \tag{20}$$

where $|\Psi\rangle$ is an arbitrary M-mode bosonic state and $\hat{U}_G^{\mathrm{Enc}}$ is a Gaussian unitary operation (see Fig. 6 for the encoding circuit). For example, for the N-mode GKP-repetition code we have $M = 1$ and $\hat{U}_G^{\mathrm{Enc}} = \prod_{k=2}^{N} \mathrm{SUM}_{1 \to k}$, and for the two-mode GKP-squeezed-repetition code $M = 1$, $N = 2$ and $\hat{U}_G^{\mathrm{Enc}} = \mathrm{Sq}_1(1/\lambda)\mathrm{Sq}_2(\lambda)\mathrm{SUM}_{1 \to 2}$. Since one can choose any Gaussian operation as an encoding circuit $\hat{U}_G^{\mathrm{Enc}}$, our GKP-stabilizer formalism is at least as flexible as the stabilizer formalism for DV quantum error-correcting codes [58] which encompasses almost all conventional multi-qubit QEC schemes. Therefore, our GKP-stabilizer formalism has a great deal of potential. For example, one can concatenate the two-mode GKP-squeezed-repetition codes and define a four-mode GKP-stabilizer code that can suppress additive Gaussian noise errors to the fourth order, i.e., $\sigma \to \sigma^4$ (or even more generally, $\sigma \to \sigma^N$ using $N = 2^l$ modes with a higher level of concatenation where $l \in \mathbb{N}$). In addition, it will also be interesting to consider an encoding circuit $\hat{U}_G^{\mathrm{Enc}}$ which is analogous to the encoding circuit of a multi-qubit surface code [59, 60] and define a CV-into-CV GKP-surface code which can be implemented locally on a 2-dimensional plane (see Ref. [20] for the DV-into-CV Toric-GKP code).

We leave finding useful GKP-stabilizer codes by exploring various Gaussian encoding circuits $\hat{U}_G^{\mathrm{Enc}}$ as a future research direction. Here, we instead provide a general decoding strategy for a general GKP-stabilizer code. Consider a general symplectic matrix $\boldsymbol{S}$ associated with the Gaussian encoding circuit $\hat{U}_G^{\mathrm{Enc}}$. Since $\boldsymbol{S}$ is a symplectic matrix, $\boldsymbol{S\Omega S}^T = \boldsymbol{\Omega}$ holds where $\boldsymbol{\Omega}$ is given by

$$\boldsymbol{\Omega} = \begin{bmatrix} \boldsymbol{\omega} & & \\ & \ddots & \\ & & \boldsymbol{\omega} \end{bmatrix} \text{ and } \boldsymbol{\omega} = \begin{bmatrix} 0 & 1 \\ -1 & 0 \end{bmatrix} \tag{21}$$

(see, for example, Ref. [2]). Then, following the same reasoning as in Subsection IV A, we obtain the reshaped quadrature noise vector $\boldsymbol{z} \equiv (z_q^{(1)}, z_p^{(1)}, \cdots, z_q^{(N)}, z_p^{(N)})^T = \boldsymbol{S}^{-1}\boldsymbol{\xi}$ as a result of the encoding, additive Gaussian noise errors and the inverse of the encoding circuit where $\boldsymbol{\xi} \equiv (\xi_q^{(1)}, \xi_p^{(1)}, \cdots, \xi_q^{(N)}, \xi_p^{(N)})^T$ is the original quadrature noise vector. Let us write $\boldsymbol{z} = \boldsymbol{S}^{-1}\boldsymbol{\xi}$ more explicitly as follows:

$$\begin{bmatrix} \boldsymbol{z_x} \\ \boldsymbol{z_y} \end{bmatrix} = \begin{bmatrix} (\boldsymbol{S}^{-1})_{xx} & (\boldsymbol{S}^{-1})_{xy} \\ (\boldsymbol{S}^{-1})_{yx} & (\boldsymbol{S}^{-1})_{yy} \end{bmatrix} \begin{bmatrix} \boldsymbol{\xi_x} \\ \boldsymbol{\xi_y} \end{bmatrix}. \tag{22}$$

Here, the subscript $\boldsymbol{x}$ is associated with the data modes (i.e., the first M modes) and the subscript $\boldsymbol{y}$ is associated with the ancilla modes (i.e., the last $N - M$ modes). That is, $\boldsymbol{z_x} = (z_q^{(1)}, z_p^{(1)}, \cdots, z_q^{(M)}, z_p^{(M)})^T$, $\boldsymbol{z_y} = (z_q^{(M+1)}, z_p^{(M+1)}, \cdots, z_q^{(N)}, z_p^{(N)})^T$ and the same applies to $\boldsymbol{\xi_x}$ and $\boldsymbol{\xi_y}$. Also, $(\boldsymbol{S}^{-1})_{xx}$, $(\boldsymbol{S}^{-1})_{xy}$, $(\boldsymbol{S}^{-1})_{yx}$ and $(\boldsymbol{S}^{-1})_{yy}$ are $2M \times 2M$, $2M \times 2(N-M)$, $2(N-M) \times 2M$ and $2(N-M) \times 2(N-M)$ matrices, respectively.
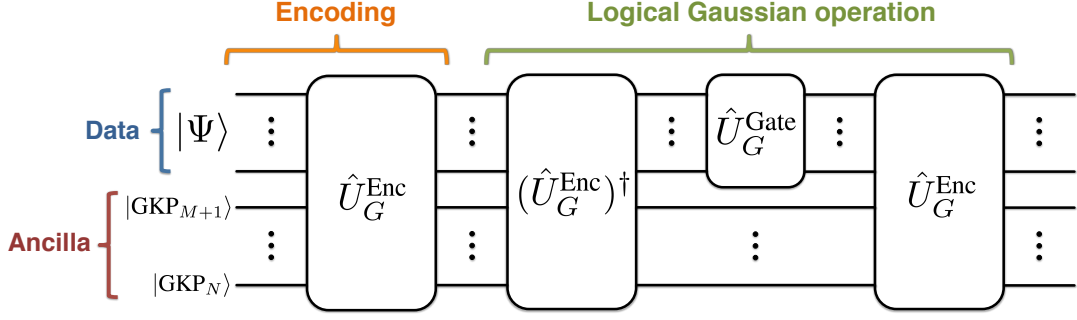
FIG. 6: Encoding circuit of a general GKP-stabilizer code and implementation of a general logical Gaussian operation.

After applying the inverse of the encoding circuit, we measure each component of the reshaped ancilla quadrature noise vector $z_y = (S^{-1})_{yx}\xi_x + (S^{-1})_{yy}\xi_y$ modulo $\sqrt{2\pi}$. For now, we ignore the fact that we can measure each component of z_y only modulo $\sqrt{2\pi}$ and assume that we know its exact value. Based on the extracted syndrome measurement outcome z_y, we can infer that

$$\xi_y = -A_{yx}\xi_x + B_{yy}z_y, \qquad (23)$$

where $A_{yx} \equiv ((S^{-1})_{yy})^{-1}(S^{-1})_{yx}$ and $B_{yy} \equiv ((S^{-1})_{yy})^{-1}$. Then, since a noise vector ξ with smaller $|\xi|^2 = \xi_x^T\xi_x + \xi_y^T\xi_y$ is more likely, we estimate that ξ_x is

$$\bar{\xi}_x = \mathrm{argmin}_{\xi_x}\Big[\xi_x^T\xi_x$$
$$+ (-\xi_x^T(A_{yx})^T + z_y^T(B_{yy})^T)(-A_{yx}\xi_x + B_{yy}z_y)\Big]$$
$$= (I_x + (A_{yx})^T A_{yx})^{-1}(A_{yx})^T B_{yy}z_y, \qquad (24)$$

where I_x is the $2M \times 2M$ identity matrix. Finally, since we can only measure z_y modulo $\sqrt{2\pi}$, we replace z_y by $\bar{z}_y \equiv R_{\sqrt{2\pi}}(z_y)$ and obtain the following estimate:

$$\tilde{\xi}_x = (I_x + (A_{yx})^T A_{yx})^{-1}(A_{yx})^T B_{yy}\bar{z}_y,$$
$$\tilde{\xi}_y = -A_{yx}\tilde{\xi}_x + B_{yy}\bar{z}_y. \qquad (25)$$

We remark that the estimates in Eqs. (8),(16) are special cases of Eq. (25). We observe that this decoding procedure is computationally efficient because it only involves multiplications and inversions of matrices of size at most $2N \times 2N$, where N is the number of the physical bosonic modes.

Finally we remark that, for any GKP-stabilizer code, any logical Gaussian operation $(\hat{U}_G^{\mathrm{Gate}})_L$ can be readily implemented by using only physical Gaussian operations $\hat{U}_G^{\mathrm{Enc}}(\hat{U}_G^{\mathrm{Gate}} \otimes \hat{I}_{N-M})(\hat{U}_G^{\mathrm{Enc}})^\dagger$ (see Fig. 6). This is because the input GKP states $|\mathrm{GKP}_{M+1}\rangle, \cdots, |\mathrm{GKP}_N\rangle$ are the only non-Gaussian resources in the encoding scheme and the remaining circuit $\hat{U}_G^{\mathrm{Enc}}$ is Gaussian. For example, logical displacement operations, squeezing operations and beam splitter interactions can be implemented by using only physical Gaussian operations. Thus, our GKP-stabilizer codes will be useful for realizing *error-corrected* boson sampling [3] and simula-

tion of vibrational quantum dynamics of molecules [4, 5].

V. DISCUSSION

In this section, we briefly discuss experimental realization of our GKP-stabilizer codes and the effects of realistic imperfections. Recall that the only required non-Gaussian resource for implementing GKP-stabilizer codes is the preparation of a canonical GKP state. Recently, approximate GKP states have been realized experimentally in a trapped ion system [25, 26] by using a heralded preparation scheme with post-selection [42] and also in a circuit QED system [27] by using a deterministic preparation scheme without post-selection [27, 46]. In this regard, we emphasize that our GKP-stabilizer coding schemes are compatible with both the deterministic and non-deterministic preparation schemes. This is because the required GKP states can be prepared offline and then injected into the error correction circuit in the middle of the decoding procedure (similar to the magic state and magic state injection for universal DV quantum computation [61]).

We remark that near-term applications of our GKP-stabilizer QEC schemes will be mainly limited by the imperfections in GKP states such as their finite photon number and limited fidelity. In this regime, since our GKP-stabilizer coding schemes are compatible with any non-deterministic GKP state preparation scheme, it will be more advantageous to sacrifice the success probability of a GKP state preparation scheme and aim to prepare a GKP state of higher quality (with a larger photon number and higher fidelity) by using post-selection, as opposed to deterministically preparing a GKP state of lower quality.

The imperfections in GKP states can be especially detrimental to the implementation of a GKP-stabilizer code involving a large squeezing parameter because such imperfections may be significantly amplified by the large squeezing operations. With this concern in mind, let us revisit the two-mode GKP-squeezed-repetition code in Subsection IV A and recall that the choice of the squeezing parameter $\lambda = \sqrt{2\pi}c/\sigma$ (with a small constant $c \ll 1$) was essential for achieving the quadratic suppression of additive Gaussian noise errors. If the standard deviation of the input noise is very small (i.e., $\sigma \ll \sqrt{2\pi}c$), we do indeed have a huge squeezing parameter $\lambda \gg 1$. However, we emphasize that we have designed

the two-mode GKP-squeezed-repetition code very carefully so that any imperfections in GKP states are not amplified by the large squeezing operations: We elaborate more on this below.

Note that the imperfections in GKP states will introduce additional noises during the syndrome extraction procedure. To be more specific, the estimated reshaped ancilla quadrature noises in Eq. (15) will be corrupted as

$$\bar{z}_q^{(2)} = R_{\sqrt{2\pi}}(z_q^{(2)} + \delta_q^{\text{GKP}}),$$
$$\bar{z}_p^{(2)} = R_{\sqrt{2\pi}}(z_p^{(2)} + \delta_p^{\text{GKP}}), \tag{26}$$

where the additional noises δ_q^{GKP} and δ_p^{GKP} are due to, for example, the finite size and infidelity of the GKP states supplied to the error correction cycle. Such additional noise will then be propagated to the data mode through the miscalibrated counter displacement operations based on noisy estimates. Note, however, that the sizes of the counter displacements $\exp[i\hat{p}_1\lambda\tilde{\xi}_q^{(1)}]$ and $\exp[-i\hat{q}_1\lambda\tilde{\xi}_p^{(2)}]$

$$\lambda\tilde{\xi}_q^{(1)} = -\frac{\lambda^4}{1+\lambda^4}\bar{z}_q^{(2)} \xrightarrow{\lambda \gg 1} -\bar{z}_q^{(2)},$$
$$\lambda\tilde{\xi}_p^{(1)} = \bar{z}_p^{(2)} \tag{27}$$

do not explicitly depend on λ in the $\lambda \gg 1$ limit (see Eq. (16)). Therefore, the additional GKP noises δ_q^{GKP} and δ_p^{GKP} will simply be added to the data quadrature noises *without* being amplified by the large squeezing parameter $\lambda \gg 1$. This absence of the noise amplification is a feature of our scheme and is generally not the case for a generic GKP-stabilizer code involving large squeezing operations. Therefore, the avoidance of the GKP noise amplification should be carefully taken into account in the design of GKP-stabilizer codes.

Finally, we outline several open questions. First, continuing the discussion of imperfect GKP states, it remains to be answered if there exists a family of fault-tolerant GKP-stabilizer codes where the added noise from GKP states mentioned above can be suppressed arbitrarily as the system size increases when the imperfections are below a certain noise threshold. Moreover, it will be an interesting research avenue to search for a family of efficient GKP-stabilizer codes by exploring various encoding circuits $\hat{U}_G^{\text{Enc}}$. For example, one can look for GKP-stabilizer codes that can be implemented locally in a low dimensional space, or for ones with low resource overheads, or ones with high fault-tolerant threshold, if any. In addition, while logical Gaussian operations can be readily implemented by using only Gaussian operations for any GKP-stabilizer codes, implementation of logical non-Gaussian operations will require some non-Gaussian resources. Thus, it will also be interesting to explore whether logical non-Gaussian operations can be implemented efficiently by using, e.g., GKP states or cubic phase states as non-Gaussian resources.

VI. CONCLUSION

We have worked around the previous no-go theorems on Gaussian QEC schemes [20, 35, 36] and proposed several CV-into-CV non-Gaussian QEC schemes, GKP-repetition codes and the two-mode GKP-squeezed-repetition code, that can correct additive Gaussian noise errors. We generalized them to an even broader class of non-Gaussian QEC codes, namely, GKP-stabilizer codes. We also showed that our proposed QEC schemes can also correct excitation losses and thermal noise as well as additive Gaussian noise errors by a suitable noise conversion through a quantum-limited amplification channel. The only required non-Gaussian resource for our GKP-stabilizer QEC schemes is the preparation of the canonical GKP state. We showed that, for any GKP-stabilizer codes, logical Gaussian operations can be readily implemented by using only physical Gaussian operations. Therefore, our GKP-stabilizer QEC schemes will be useful for realizing error-corrected boson sampling and simulation of bosonic systems. In addition, our GKP-stabilizer QEC schemes may also be able to suppress errors for quantum metrology with bosonic sensors, avoid the need for CV-DV-CV conversion for quantum communication over bosonic channels and enable fault-tolerant universal CV quantum computing.

Appendix A: Gaussian-repetition codes

Here, we introduce and analyze the N-mode Gaussian-repetition code, which is a straightforward generalization of the three-mode Gaussian-repetition code introduced in Refs. [28, 29]. In particular, we introduce the maximum likelihood estimation of the data position quadrature noise $\xi_q^{(1)}$ for the N-mode Gaussian-repetition code, which is a key motivation behind our choice of the estimate $\tilde{\xi}_q^{(1)}$ given in Eq. (9).

Consider an arbitrary oscillator state $|\psi\rangle = \int dq\psi(q)|\hat{q}_1 = q\rangle$. The state $|\psi\rangle$ can be embedded in N oscillator modes via the N-mode Gaussian-repetition code as follows:

$$|\psi_L\rangle = \int dq\psi(q)\bigotimes_{k=1}^{N}|\hat{q}_k = q\rangle, \tag{A1}$$

where the first mode is the data mode and the rest are the ancilla modes. Note that the data position eigenstate $|\hat{q}_1 = q\rangle$ is
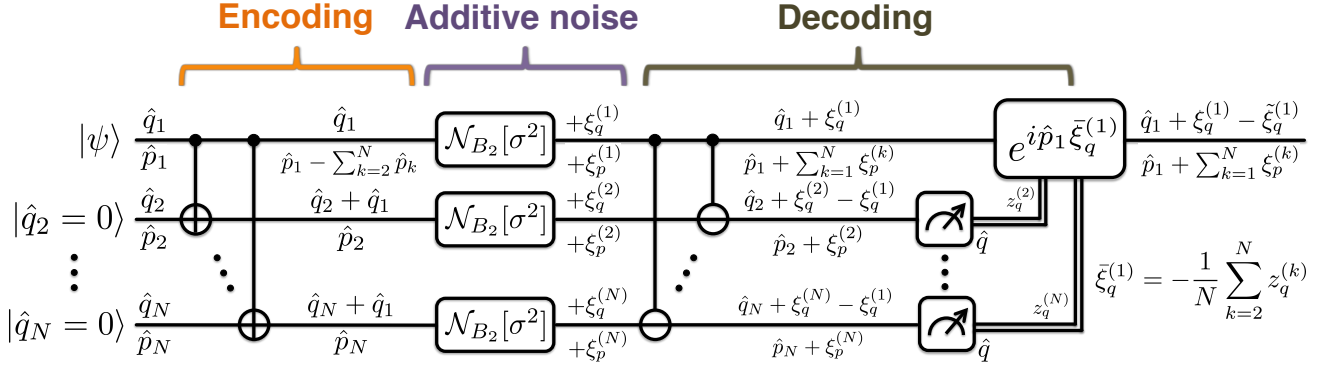
FIG. 7: Encoding and decoding circuits of the N-mode GKP-repetition code, subject to independent and identically distributed additive Gaussian noise errors.

mapped into $\bigotimes_{k=1}^{N} |\hat{q}_k = q\rangle$ through the encoding procedure. As shown in Fig. 7, this encoding can be realized by applying a sequence of Gaussian SUM gates $\text{SUM}_{1\to k} \equiv \exp[-i\hat{q}_1\hat{p}_k]$ where $k \in \{2, \cdots, N\}$. Upon the encoding circuit, the quadrature operators are transformed into

$$\hat{q}_1 \to \hat{q}_1' \equiv \hat{q}_1, \qquad \hat{p}_1 \to \hat{p}_1' \equiv \hat{p}_1 - \sum_{k=2}^{N} \hat{p}_k,$$

$$\hat{q}_k \to \hat{q}_k' \equiv \hat{q}_k + \hat{q}_1, \quad \hat{p}_k \to \hat{p}_k' \equiv \hat{p}_k, \qquad (A2)$$

as in Eq. (4) where $k \in \{2, \cdots, N\}$. We then assume that the oscillator modes undergo independent and identically distributed additive Gaussian noise errors $\mathcal{N} = \bigotimes_{k=1}^{N} \mathcal{N}_{B_2}^{(k)}[\sigma^2]$, i.e.,

$$\hat{q}_k' \to \hat{q}_k'' \equiv \hat{q}_k' + \xi_q^{(k)} \text{ and } \hat{p}_k' \to \hat{p}_k'' \equiv \hat{p}_k' + \xi_p^{(k)}, \quad (A3)$$

as in Eq. (5). The added noises $\xi_{q/p}^{(1)}, \cdots, \xi_{q/p}^{(N)}$ follow an independent and identically distributed Gaussian random distribution $(\xi_q^{(1)}, \xi_p^{(1)}, \cdots, \xi_q^{(N)}, \xi_p^{(N)}) \sim_{\text{iid}} \mathcal{N}(0, \sigma^2)$.

The goal of the decoding procedure (shown in Fig. 7) is to extract some information about the added noises $\xi_q^{(k)}$ and $\xi_p^{(k)}$ ($k \in \{1, \cdots, N\}$) through a set of syndrome measurements. The decoding procedure begins with the inverse of the encoding circuit, i.e., by a sequence of DIFFERENCE gates $\text{DIFFERENCE}_{1\to k} \equiv \exp[i\hat{q}_1\hat{p}_k]$ for $k \in \{2, \cdots, N\}$. Upon the inverse of the encoding circuit, the quadrature operators are transformed into $\hat{q}_k'' \to \hat{q}_k + z_q^{(k)}$ and $\hat{p}_k'' \to \hat{p}_k + z_p^{(k)}$, where the reshaped quadrature noises are given by

$$z_q^{(1)} \equiv \xi_q^{(1)}, \qquad z_p^{(1)} \equiv \sum_{k=1}^{N} \xi_p^{(k)},$$

$$z_q^{(k)} \equiv \xi_q^{(k)} - \xi_q^{(1)}, \qquad z_p^{(k)} \equiv \xi_p^{(k)}, \qquad (A4)$$

as in Eq. (7) where $k \in \{2, \cdots, N\}$. Then, by performing homodyne measurements of the ancilla position quadrature op-

erators, we can exactly extract the values of

$$z_q^{(k)} = \xi_q^{(k)} - \xi_q^{(1)} \qquad (A5)$$

for all $k \in \{2, \cdots, N\}$. This is because the ancilla modes are initially in the position eigenstates $|\hat{q}_k = 0\rangle$ and thus measuring $\hat{q}_k''' = \hat{q}_k + z_q^{(k)}$ is equivalent to measuring $z_q^{(k)}$ for all $k \in \{2, \cdots, N\}$. Note, however, that we cannot extract any information about the reshaped momentum quadrature noises $z_p^{(1)}, \cdots, z_p^{(N)}$. This will later turn out to be the key limitation of Gaussian-repetition codes.

From the extracted values of $z_q^{(k)} = \xi_q^{(k)} - \xi_q^{(1)}$, we can infer that position quadrature noises are given by $\vec{\xi}_q \equiv (\xi_q^{(1)}, \xi_q^{(2)}, \cdots, \xi_q^{(N)}) = (\xi_q^{(1)}, \xi_q^{(1)} + z_q^{(2)}, \cdots, \xi_q^{(1)} + z_q^{(N)})$. Then, the undetermined data position quadrature noise $\xi_q^{(1)}$ can be estimated by a maximum likelihood estimation: Since noises with smaller $|\vec{\xi}_q|^2 \equiv \sum_{k=1}^{N} (\xi_q^{(k)})^2$ are more likely, we estimate that $\xi_q^{(1)}$ is

$$\bar{\xi}_q^{(1)} = \text{argmin}_{\xi_q^{(1)}} \left[(\xi_q^{(1)})^2 + \sum_{k=2}^{N} (\xi_q^{(1)} + z_q^{(k)})^2 \right]$$

$$= -\frac{1}{N} \sum_{k=2}^{N} z_q^{(k)} \qquad (A6)$$

from the syndrome measurement outcomes $z_q^{(2)}, \cdots, z_q^{(N)}$. This is the main reason why we chose $\tilde{\xi}_q^{(1)}$ in Eq. (9) in the main text as the estimate of $\xi_q^{(1)}$. Finally, the decoding procedure ends with an application of the counter displacement operation $\exp[i\hat{p}_1\bar{\xi}_q^{(1)}]$ to the data oscillator mode (see Fig. 7).

As a result of the encoding and decoding procedures, we end up with a logical additive noise error $\hat{q}_1 \to \hat{q}_1 + \xi_q$ and $\hat{p}_1 \to \hat{p}_1 + \xi_p$ of the data oscillator mode, where the logical

quadrature noises are given by

$$\xi_q \equiv z_q^{(1)} - \bar{\xi}_q^{(1)} = \frac{1}{N}\sum_{k=1}^{N}\xi_q^{(k)},$$

$$\xi_p \equiv z_p^{(1)} = \sum_{k=1}^{N}\xi_p^{(k)}. \tag{A7}$$

Since $(\xi_q^{(1)}, \xi_p^{(1)}, \cdots, \xi_q^{(N)}, \xi_p^{(N)}) \sim_{\text{iid}} \mathcal{N}(0, \sigma^2)$, we have

$$\xi_q = \frac{1}{N}\sum_{k=1}^{N}\xi_q^{(k)} \sim \mathcal{N}\left(0, \sigma_q^2 \equiv \frac{1}{N}\sigma^2\right),$$

$$\xi_p = \sum_{k=1}^{N}\xi_p^{(k)} \sim \mathcal{N}\left(0, \sigma_p^2 \equiv N\sigma^2\right). \tag{A8}$$

Thus, the variance of the position quadrature noise is reduced by a factor of N, but the variance of the momentum quadrature noise is increased by the same factor. The latter increase is due to the fact that the ancilla momentum quadrature noises which are transferred to the data momentum quadrature (see $+\sum_{k=2}^{N}\xi_p^{(k)}$ in $z_p^{(1)}$) are left completely undetected by the position homodyne measurements during the syndrome extraction stage. As a result, the product of the noise standard deviations remains unchanged at the end of the error correction procedure (i.e., $\sigma_q\sigma_p = \sigma^2$). This implies that Gaussian-repetition codes can only squeeze the Gaussian quadrature noises but cannot actually correct them. This reaffirms the previous no-go results [20, 35, 36].

In Section III in the main text, we modify these Gaussian-repetition codes and introduce a family of GKP-repetition codes that can indeed correct additive Gaussian noise errors. Specifically, we replace several Gaussian elements in the Gaussian-repetition code by non-Gaussian ones involving the canonical GKP state, such that we can only benefit from the decreased position noise variance by a factor of N, while preventing the momentum noise variance from increasing by the same factor.

Appendix B: Probability density of the logical quadrature noises: GKP-repetition codes

Here, we provide explicit expressions for the probability density functions of the logical quadrature noises ξ_q and ξ_p

for the N-mode GKP-repetition code, which are given in Eq. (10) in the main text. Recall that the logical quadrature noises ξ_q and ξ_p for the N-mode GKP-repetition are given by

$$\xi_q = \xi_q^{(1)} + \frac{1}{N}\sum_{k=2}^{N}R_{\sqrt{2\pi}}(\xi_q^{(k)} - \xi_q^{(1)}),$$

$$\xi_p = \xi_p^{(1)} + \sum_{k=2}^{N}(\xi_p^{(k)} - R_{\sqrt{2\pi}}(\xi_p^{(k)})), \tag{B1}$$

where $(\xi_q^{(1)}, \xi_p^{(1)}, \cdots, \xi_q^{(N)}, \xi_p^{(N)}) \sim_{\text{iid}} \mathcal{N}(0, \sigma^2)$ and $R_s(z) \equiv z - n^\star(z)s$ and $n^\star(z) \equiv \text{argmin}_{n\in\mathbb{Z}}|z - ns|$. Let $p_\sigma(z)$ denote the probability density function of a Gaussian distribution with zero mean and variance σ^2, i.e., $p_\sigma(z) \equiv (1/\sqrt{2\pi\sigma^2})\exp[-z^2/(2\sigma^2)]$. Then, the probability density functions $Q(\xi_q)$ and $P(\xi_p)$ of the logical quadrature noises ξ_q and ξ_p are given by

$$Q(\xi_q) \equiv \int_{-\infty}^{\infty}d\xi_q^{(1)}\cdots\int_{-\infty}^{\infty}d\xi_q^{(N)}\Big[\prod_{k=1}^{N}p_\sigma(\xi_q^{(k)})\Big]$$

$$\times \delta\Big(\xi_q - \xi_q^{(1)} - \frac{1}{N}\sum_{k=2}^{N}R_{\sqrt{2\pi}}(\xi_q^{(k)} - \xi_q^{(1)})\Big), \tag{B2}$$

and

$$P(\xi_p) \equiv \int_{-\infty}^{\infty}d\xi_p^{(1)}\cdots\int_{-\infty}^{\infty}d\xi_p^{(N)}\Big[\prod_{k=1}^{N}p_\sigma(\xi_p^{(k)})\Big]$$

$$\times \delta\Big(\xi_p - \xi_p^{(1)} - \sum_{k=2}^{N}(\xi_p^{(k)} - R_{\sqrt{2\pi}}(\xi_p^{(k)}))\Big), \tag{B3}$$

where $\delta(x)$ is the Dirac delta function. Note that $R_s(z)$ can be expressed as

$$R_s(z) \equiv \sum_{n\in\mathbb{Z}}(z - ns)\cdot I\Big\{z \in \Big[\Big(n - \frac{1}{2}\Big)s, \Big(n + \frac{1}{2}\Big)s\Big]\Big\}, \tag{B4}$$

where $I\{C\}$ is an indicator function, i.e., $I\{C\} = 1$ if C is true $I\{C\} = 0$ if C is false. Then, using Eq. (B4), we can make $Q(\xi_q)$ and $P(\xi_p)$ in Eqs. (B2),(B3) more explicit as follows:

$$Q(\xi_q) = \sum_{n_2,\cdots,n_n \in \mathbb{Z}} \int_{-\infty}^{\infty} d\xi_q^{(1)} \cdots \int_{-\infty}^{\infty} d\xi_q^{(N)} \Big[\prod_{k=1}^{N} p_\sigma(\xi_q^{(k)}) \Big] \delta\Big(\xi_q - \xi_q^{(1)} - \frac{1}{N}\sum_{k=2}^{N}\big(\xi_q^{(k)} - \xi_q^{(1)} - \sqrt{2\pi}\,n_k\big)\Big)$$

$$\times \Big[\prod_{k=2}^{N} I\Big\{ \xi_q^{(k)} - \xi_q^{(1)} \in \Big[\big(n_k - \frac{1}{2}\big)\sqrt{2\pi}, \big(n_k + \frac{1}{2}\big)\sqrt{2\pi}\Big] \Big\} \Big]$$

$$= \sum_{n_2,\cdots,n_n \in \mathbb{Z}} \Big[\prod_{k=2}^{N} \int_{-\sqrt{\pi/2}}^{\sqrt{\pi/2}} d\xi_q^{(k)} \Big] p_\sigma\Big(\xi_q - \frac{1}{N}\sum_{k=2}^{N}\xi_q^{(k)}\Big)\Big[\prod_{k=2}^{N} p_\sigma\Big(\xi_q^{(k)} + \xi_q - \frac{1}{N}\sum_{\ell=2}^{N}\xi_q^{(\ell)} + \sqrt{2\pi}\,n_k\Big)\Big], \qquad \text{(B5)}$$

and

$$P(\xi_p) = \sum_{n_2,\cdots,n_n \in \mathbb{Z}} \int_{-\infty}^{\infty} d\xi_p^{(1)} \cdots \int_{-\infty}^{\infty} d\xi_p^{(N)} \Big[\prod_{k=1}^{N} p_\sigma(\xi_p^{(k)}) \Big] \delta\Big(\xi_p - \xi_p^{(1)} - \sqrt{2\pi}\sum_{k=2}^{N} n_k\Big)$$

$$\times \Big[\prod_{k=2}^{N} I\Big\{ \xi_p^{(k)} \in \Big[\big(n_k - \frac{1}{2}\big)\sqrt{2\pi}, \big(n_k + \frac{1}{2}\big)\sqrt{2\pi}\Big] \Big\} \Big]$$

$$= \sum_{n_2,\cdots,n_n \in \mathbb{Z}} \Big[\prod_{k=2}^{N} \int_{\sqrt{2\pi}(n_k - \frac{1}{2})}^{\sqrt{2\pi}(n_k + \frac{1}{2})} d\xi_p^{(k)} \cdot p_\sigma(\xi_p^{(k)}) \Big] p_\sigma\Big(\xi_p - \sqrt{2\pi}\sum_{k=2}^{N} n_k\Big). \qquad \text{(B6)}$$

Fig. 3 in the main text is obtained by numerically computing these probability density functions and then evaluating the standard deviations of the obtained probability density functions.

Appendix C: Probability density of the logical quadrature noises: The two-mode GKP-squeezed-repetition code

Here, we first show that the maximum likelihood argument yields the estimate $\lambda\tilde{\xi}_q^{(1)}$ in Eq. (16) for the two-mode GKP-squeezed-repetition code. Recall that we extract the value of $z_q^{(2)} = -\lambda\xi_q^{(1)} + \xi_q^{(2)}/\lambda$ modulo $\sqrt{2\pi}$. For now, let us ignore the fact that we can measure $z_q^{(2)}$ only modulo $\sqrt{2\pi}$ and assume that we know its exact value. Then, we can infer that the position quadrature noises are given by $\vec{\xi}_q = (\xi_q^{(1)}, \xi_q^{(2)}) = (\xi_q^{(1)}, \lambda^2\xi_q^{(1)} + \lambda z_q^{(2)})$. Since noises with

smaller $|\vec{\xi}_q|^2$ are more likely, we estimate that $\xi_q^{(1)}$ is

$$\bar{\xi}_q^{(1)} = \text{argmin}_{\xi_q^{(1)}} \Big[(\xi_q^{(1)})^2 + (\lambda^2\xi_q^{(1)} + \lambda z_q^{(2)})^2 \Big]$$

$$= -\frac{\lambda^3}{1+\lambda^4} z_q^{(2)}. \qquad \text{(C1)}$$

Since we only know the value of $z_q^{(2)}$ modulo $\sqrt{2\pi}$, we can replace $z_q^{(2)}$ in Eq. (C1) by $\bar{z}_q^{(2)} = R_{\sqrt{2\pi}}(z_q^{(2)})$ and end up with the estimate $\lambda\tilde{\xi}_q^{(1)}$ given in Eq. (16).

Now we provide explicit expression for the probability density functions of the logical quadrature noises ξ_q and ξ_p for the two-mode GKP-squeezed-repetition code. Recall Eq. (17):

$$\xi_q = \lambda\xi_q^{(1)} + \frac{\lambda^4}{1+\lambda^4} R_{\sqrt{2\pi}}\Big(\frac{\xi_q^{(2)}}{\lambda} - \lambda\xi_q^{(1)}\Big),$$

$$\xi_p = \frac{\xi_p^{(1)}}{\lambda} + \lambda\xi_p^{(2)} - R_{\sqrt{2\pi}}(\lambda\xi_p^{(2)}), \qquad \text{(C2)}$$

where $(\xi_q^{(1)}, \xi_p^{(1)}, \xi_q^{(2)}, \xi_p^{(2)}) \sim_{\text{iid}} \mathcal{N}(0, \sigma^2)$. Similarly as in Appendix B, using Eq. (B4), we find that the probability density functions of the quadrature noises are given by

$$Q(\xi_q) \equiv \int_{-\infty}^{\infty} d\xi_q^{(1)} \int_{-\infty}^{\infty} d\xi_q^{(2)} p_\sigma(\xi_q^{(1)}) p_\sigma(\xi_q^{(2)}) \delta\Big(\xi_q - \lambda\xi_q^{(1)} - \frac{\lambda^4}{1+\lambda^4} R_{\sqrt{2\pi}}\Big(\frac{\xi_q^{(2)}}{\lambda} - \lambda\xi_q^{(1)}\Big)\Big)$$

$$= \sum_{n_2 \in \mathbb{Z}} \int_{-\infty}^{\infty} d\xi_q^{(1)} \int_{-\infty}^{\infty} d\xi_q^{(2)} p_\sigma(\xi_q^{(1)}) p_\sigma(\xi_q^{(2)}) \delta\Big(\xi_q - \lambda\xi_q^{(1)} - \frac{\lambda^4}{1+\lambda^4}\Big(\frac{\xi_q^{(2)}}{\lambda} - \lambda\xi_q^{(1)} - \sqrt{2\pi}n_2\Big)\Big)$$

$$\times I\Big\{\frac{\xi_q^{(2)}}{\lambda} - \lambda\xi_q^{(1)} \in \Big[\Big(n_2 - \frac{1}{2}\Big)\sqrt{2\pi}, \Big(n_2 + \frac{1}{2}\Big)\sqrt{2\pi}\Big]\Big\}$$

$$= \sum_{n_2 \in \mathbb{Z}} \int_{-\sqrt{\pi/2}}^{\sqrt{\pi/2}} d\xi_q^{(2)} p_\sigma\Big(\frac{\xi_q}{\lambda} - \frac{\lambda^3}{1+\lambda^4}\xi_q^{(2)}\Big) p_\sigma\Big(\lambda\xi_q^{(2)} + \lambda\xi_q - \frac{\lambda^5}{1+\lambda^4}\xi_q^{(2)} + \sqrt{2\pi}\lambda n_2\Big), \tag{C3}$$

and

$$P(\xi_p) \equiv \int_{-\infty}^{\infty} d\xi_p^{(1)} \int_{-\infty}^{\infty} d\xi_p^{(2)} p_\sigma(\xi_p^{(1)}) p_\sigma(\xi_p^{(2)}) \delta\Big(\xi_p - \frac{\xi_p^{(1)}}{\lambda} - (\lambda\xi_p^{(2)} - R_{\sqrt{2\pi}}(\lambda\xi_p^{(2)}))\Big)$$

$$= \sum_{n_2 \in \mathbb{Z}} \int_{-\infty}^{\infty} d\xi_p^{(1)} \int_{-\infty}^{\infty} d\xi_p^{(2)} p_\sigma(\xi_p^{(1)}) p_\sigma(\xi_p^{(2)}) \delta\Big(\xi_p - \frac{\xi_p^{(1)}}{\lambda} - \sqrt{2\pi}n_2\Big)$$

$$\times I\Big\{\lambda\xi_p^{(2)} \in \Big[\Big(n_2 - \frac{1}{2}\Big)\sqrt{2\pi}, \Big(n_2 + \frac{1}{2}\Big)\sqrt{2\pi}\Big]\Big\}$$

$$= \sum_{n_2 \in \mathbb{Z}} \Big[\int_{-\sqrt{2\pi}(n_2-\frac{1}{2})}^{\sqrt{2\pi}(n_2-\frac{1}{2})} d\xi_p^{(2)} p_\sigma\Big(\frac{\xi_p^{(2)}}{\lambda}\Big)\Big] p_\sigma\Big(\lambda\xi_p - \sqrt{2\pi}\lambda n_2\Big). \tag{C4}$$

Fig. 5 in the main text is obtained by numerically computing these probability density functions and then evaluating the standard deviations of the obtained probability density functions.

---

[1] S. L. Braunstein and P. van Loock, "Quantum information with continuous variables," Rev. Mod. Phys. **77**, 513–577 (2005).

[2] C. Weedbrook, S. Pirandola, R. García-Patrón, N. J. Cerf, T. C. Ralph, J. H. Shapiro, and S. Lloyd, "Gaussian quantum information," Rev. Mod. Phys. **84**, 621–669 (2012).

[3] S. Aaronson and A. Arkhipov, "The computational complexity of linear optics," in *Proceedings of the Forty-third Annual ACM Symposium on Theory of Computing*, STOC '11 (ACM, New York, NY, USA, 2011) pp. 333–342.

[4] J. Huh, G. G. Guerreschi, B. Peropadre, J. R. McClean, and A. Aspuru-Guzik, "Boson sampling for molecular vibronic spectra," Nature Photonics **9**, 615–620 (2015).

[5] C. Sparrow, E. Martín-López, N. Maraviglia, A. Neville, C. Harrold, J. Carolan, Y. N. Joglekar, T. Hashimoto, N. Matsuda, J. L. O'Brien, D. P. Tew, and A. Laing, "Simulating the vibrational quantum dynamics of molecules using photonics," Nature **557**, 660–667 (2018).

[6] S. Aaronson and D. J. Brod, "Bosonsampling with lost photons," Phys. Rev. A **93**, 012335 (2016).

[7] D. Gottesman, "An Introduction to Quantum Error Correction and Fault-Tolerant Quantum Computation," arXiv e-prints , arXiv:0904.2557 (2009), arXiv:0904.2557 [quant-ph].

[8] V. V. Albert, K. Noh, K. Duivenvoorden, D. J. Young, R. T. Brierley, P. Reinhold, C. Vuillot, L. Li, C. Shen, S. M. Girvin, B. M. Terhal, and Liang J., "Performance and structure of single-mode bosonic codes," Phys. Rev. A **97**, 032346 (2018).

[9] P. T. Cochrane, G. J. Milburn, and W. J. Munro, "Macroscopically distinct quantum-superposition states as a bosonic code for amplitude damping," Phys. Rev. A **59**, 2631–2634 (1999).

[10] D. Gottesman, A. Kitaev, and J. Preskill, "Encoding a qubit in an oscillator," Phys. Rev. A **64**, 012310 (2001).

[11] M. Mirrahimi, Z. Leghtas, V. V. Albert, S. Touzard, R. J. Schoelkopf, L. Jiang, and M. H. Devoret, "Dynamically protected cat-qubits: a new paradigm for universal quantum computation," New Journal of Physics **16**, 045014 (2014).

[12] M. H. Michael, M. Silveri, R. T. Brierley, V. V. Albert, J. Salmilehto, L. Jiang, and S. M. Girvin, "New class of quantum error-correcting codes for a bosonic mode," Phys. Rev. X **6**, 031006 (2016).

[13] I. L. Chuang, D. W. Leung, and Y. Yamamoto, "Bosonic quantum codes for amplitude damping," Phys. Rev. A **56**, 1114–1125 (1997).

[14] J. Harrington and J. Preskill, "Achievable rates for the Gaussian quantum channel," Phys. Rev. A **64**, 062301 (2001).

[15] M. Bergmann and P. van Loock, "Quantum error correction against photon loss using NOON states," Phys. Rev. A **94**, 012311 (2016).

[16] K. Fukui, A. Tomita, and A. Okamoto, "Analog quantum error correction with encoding a qubit into an oscillator," Phys. Rev. Lett. **119**, 180507 (2017).

[17] M. Y. Niu, I. L. Chuang, and J. H. Shapiro, "Hardware-efficient bosonic quantum error-correcting codes based on symmetry op-

erators," Phys. Rev. A **97**, 032323 (2018).

[18] K. Fukui, A. Tomita, A. Okamoto, and K. Fujii, "High-threshold fault-tolerant quantum computation with analog quantum error correction," Phys. Rev. X **8**, 021054 (2018).

[19] K. Fukui, A. Tomita, and A. Okamoto, "Tracking quantum error correction," Phys. Rev. A **98**, 022326 (2018).

[20] C. Vuillot, H. Asasi, Y. Wang, L. P. Pryadko, and B. M. Terhal, "Quantum Error Correction with the Toric-GKP Code," arXiv e-prints , arXiv:1810.00047 (2018), arXiv:1810.00047 [quant-ph].

[21] Z. Leghtas, S. Touzard, I. M. Pop, A. Kou, B. Vlastakis, A. Petrenko, K. M. Sliwa, A. Narla, S. Shankar, M. J. Hatridge, M. Reagor, L. Frunzio, R. J. Schoelkopf, M. Mirrahimi, and M. H. Devoret, "Confining the state of light to a quantum manifold by engineered two-photon loss," Science **347**, 853–857 (2015).

[22] N. Ofek, A. Petrenko, R. Heeres, P. Reinhold, Z. Leghtas, B. Vlastakis, Y. Liu, L. Frunzio, S. M. Girvin, L. Jiang, M. Mirrahimi, M. H. Devoret, and R. J. Schoelkopf, "Extending the lifetime of a quantum bit with error correction in superconducting circuits," Nature **536**, 441–445 (2016).

[23] S. Touzard, A. Grimm, Z. Leghtas, S. O. Mundhada, P. Reinhold, C. Axline, M. Reagor, K. Chou, J. Blumoff, K. M. Sliwa, S. Shankar, L. Frunzio, R. J. Schoelkopf, M. Mirrahimi, and M. H. Devoret, "Coherent oscillations inside a quantum manifold stabilized by dissipation," Phys. Rev. X **8**, 021005 (2018).

[24] L. Hu, Y. Ma, W. Cai, X. Mu, Y. Xu, W. Wang, Y. Wu, H. Wang, Y. P. Song, C.-L. Zou, S. M. Girvin, L.-M. Duan, and L. Sun, "Quantum error correction and universal gate set operation on a binomial bosonic logical qubit," Nature Physics (2019), 10.1038/s41567-018-0414-3.

[25] C. Flühmann, V. Negnevitsky, M. Marinelli, and J. P. Home, "Sequential modular position and momentum measurements of a trapped ion mechanical oscillator," Phys. Rev. X **8**, 021001 (2018).

[26] C. Flühmann, T. L. Nguyen, M. Marinelli, V. Negnevitsky, K. Mehta, and J. P. Home, "Encoding a qubit in a trapped-ion mechanical oscillator," Nature **566**, 513–517 (2019).

[27] S. Touzard, A. Eickbusch, P. Campagne-Ibarcq, E. Zalys-Geller, N. Frattini, V. Sivak, S. Puri, M. Mirrahimi, S. Shankar, and M. Devoret, "Grid states for encoding and stabilizing a logical qubit in superconducting circuits (part 2)," Bulletin of the American Physical Society (2019).

[28] S. Lloyd and J.-J. E. Slotine, "Analog Quantum Error Correction," Phys. Rev. Lett. **80**, 4088–4091 (1998).

[29] S. L. Braunstein, "Error correction for continuous quantum variables," Phys. Rev. Lett. **80**, 4084–4087 (1998).

[30] Samuel L. Braunstein, "Quantum error correction for communication with linear optics," Nature **394**, 47–49 (1998).

[31] T. Aoki, G. Takahashi, T. Kajiya, J. Yoshikawa, S. L. Braunstein, P. van Loock, and A. Furusawa, "Quantum error correction beyond qubits," Nature Physics **5**, 541 EP – (2009).

[32] P. Hayden, S. Nezami, G. Salton, and B. C. Sanders, "Space-time replication of continuous variable quantum information," New J. Phys. **18**, 083043 (2016).

[33] P. Hayden, S. Nezami, S. Popescu, and G. Salton, "Error Correction of Quantum Reference Frame Information," arXiv e-prints , arXiv:1709.04471 (2017), arXiv:1709.04471 [quant-ph].

[34] P. Faist, S. Nezami, V. V. Albert, G. Salton, F. Pastawski, P. Hayden, and J. Preskill, "Continuous symmetries and approximate quantum error correction," arXiv e-prints , arXiv:1902.07714 (2019), arXiv:1902.07714 [quant-ph].

[35] J. Eisert, S. Scheel, and M. B. Plenio, "Distilling Gaussian states with Gaussian operations is impossible," Phys. Rev. Lett. **89**, 137903 (2002).

[36] J. Niset, J. Fiurášek, and N. J. Cerf, "No-go theorem for Gaussian quantum error correction," Phys. Rev. Lett. **102**, 120501 (2009).

[37] E. Knill, R. Laflamme, and G. J. Milburn, "A scheme for efficient quantum computation with linear optics," Nature **409**, 46–52 (2001).

[38] S. Lloyd and S. L. Braunstein, "Quantum computation over continuous variables," Phys. Rev. Lett. **82**, 1784–1787 (1999).

[39] S. Krastanov, V. V. Albert, C. Shen, C.-L. Zou, R. W. Heeres, B. Vlastakis, R. J. Schoelkopf, and L. Jiang, "Universal control of an oscillator with dispersive coupling to a qubit," Phys. Rev. A **92**, 040303 (2015).

[40] B. Q. Baragiola, G. Pantaleoni, R.l N. Alexand er, A. Karanjai, and N. C. Menicucci, "All-Gaussian universality and fault tolerance with the Gottesman-Kitaev-Preskill code," arXiv e-prints , arXiv:1903.00012 (2019), arXiv:1903.00012 [quant-ph].

[41] K. Duivenvoorden, B. M. Terhal, and D. Weigand, "Single-mode displacement sensor," Phys. Rev. A **95**, 012305 (2017).

[42] B. C. Travaglione and G. J. Milburn, "Preparing encoded states in an oscillator," Phys. Rev. A **66**, 052322 (2002).

[43] S. Pirandola, S. Mancini, D. Vitali, and P. Tombesi, "Constructing finite-dimensional codes with optical continuous variables," EPL (Europhysics Letters) **68**, 323 (2004).

[44] S. Pirandola, S. Mancini, D. Vitali, and P. Tombesi, "Generating continuous variable quantum codewords in the near-field atomic lithography," Journal of Physics B: Atomic, Molecular and Optical Physics **39**, 997 (2006).

[45] H. M. Vasconcelos, L. Sanz, and S. Glancy, "All-optical generation of states for "encoding a qubit in an oscillator"," Opt. Lett. **35**, 3261–3263 (2010).

[46] B. M. Terhal and D. Weigand, "Encoding a qubit into a cavity mode in circuit QED using phase estimation," Phys. Rev. A **93**, 012315 (2016).

[47] K. R. Motes, B. Q. Baragiola, A. Gilchrist, and N. C. Menicucci, "Encoding qubits into oscillators with atomic ensembles and squeezed light," Phys. Rev. A **95**, 053819 (2017).

[48] D. J. Weigand and B. M. Terhal, "Generating grid states from Schrödinger-cat states without postselection," Phys. Rev. A **97**, 022341 (2018).

[49] J. M. Arrazola, T. R. Bromley, J. Izaac, C. R. Myers, K. Brádler, and N. Killoran, "Machine learning method for state preparation and gate synthesis on photonic quantum computers," Quantum Science and Technology **4**, 024004 (2019).

[50] D. Su, C. R.. Myers, and K. K. Sabapathy, "Conversion of Gaussian states to non-Gaussian states using photon number-resolving detectors," arXiv e-prints , arXiv:1902.02323 (2019), arXiv:1902.02323 [quant-ph].

[51] M. Eaton, R. Nehra, and O. Pfister, "Gottesman-Kitaev-Preskill state preparation by photon catalysis," arXiv e-prints , arXiv:1903.01925 (2019), arXiv:1903.01925 [quant-ph].

[52] A. S. Holevo, "One-mode quantum Gaussian channels: Structure and quantum capacity," Problems of Information Transmission **43**, 1–11 (2007).

[53] K. Noh, V. V. Albert, and L. Jiang, "Quantum capacity bounds of Gaussian thermal loss channels and achievable rates with Gottesman-Kitaev-Preskill codes," IEEE Transactions on Information Theory **65**, 2563–2582 (2019).

[54] J. Shapiro, H. Yuen, and A. Mata, "Optical communication with two-photon coherent states–part ii: Photoemissive detection and structured receiver performance," IEEE Transactions on Information Theory **25**, 179–192 (1979).

[55] M. A. Nielsen and I. L. Chuang, *Quantum Computation and*

Quantum Information, Cambridge Series on Information and the Natural Sciences (Cambridge University Press, 2000).

[56] R. Laflamme, C. Miquel, J. P. Paz, and W. H. Zurek, "Perfect quantum error correcting code," Phys. Rev. Lett. **77**, 198–201 (1996).

[57] C. H. Bennett, D. P. DiVincenzo, J. A. Smolin, and W. K. Wootters, "Mixed-state entanglement and quantum error correction," Phys. Rev. A **54**, 3824–3851 (1996).

[58] D. Gottesman, *Stabilizer codes and quantum error correction*, Ph.D. thesis, California Institute of Technology (1997).

[59] A. Kitaev, "Quantum error correction with imperfect gates," in *Quantum Communication, Computing, and Measurement*, edited by O. Hirota, A. S. Holevo, and C. M. Caves (Springer US, Boston, MA, 1997) pp. 181–188.

[60] A. G. Fowler, M. Mariantoni, J. M. Martinis, and A. N. Cleland, "Surface codes: Towards practical large-scale quantum computation," Phys. Rev. A **86**, 032324 (2012).

[61] S. Bravyi and A. Kitaev, "Universal quantum computation with ideal clifford gates and noisy ancillas," Phys. Rev. A **71**, 022316 (2005).